DEVELOPMENT OF PAPER-BASED COLORIMETRIC SENSOR FOR DETERMINATION OF
HUMAN PAPILLOMAVIRUS DNA

Miss Sarida Naorungroj

จุฬาลงกรณ์มหาวิทยาลัย
CHULALONGKORN UNIVERSITY

A Thesis Submitted in Partial Fulfillment of the Requirements
for the Degree of Master of Science in Chemistry
Department of Chemistry
FACULTY OF SCIENCE
Chulalongkorn University
Academic Year 2019
Copyright of Chulalongkorn University

การพัฒนาตัวรับรู้เชิงสีฐานกระดาษสำหรับการตรวจวัดดีเอ็นเอของเชื้อไวรัสฮิวแมนแพพิลโลมา

น.ส.สริดา เนาว์รุ่งโรจน์

วิทยานิพนธ์นี้เป็นส่วนหนึ่งของการศึกษาตามหลักสูตรปริญญาวิทยาศาสตรมหาบัณฑิต
สาขาวิชาเคมี ภาควิชาเคมี
คณะวิทยาศาสตร์ จุฬาลงกรณ์มหาวิทยาลัย
ปีการศึกษา 2562
ลิขสิทธิ์ของจุฬาลงกรณ์มหาวิทยาลัย

Thesis Title	DEVELOPMENT OF PAPER-BASED COLORIMETRIC SENSOR FOR DETERMINATION OF HUMAN PAPILLOMAVIRUS DNA
By	Miss Sarida Naorungroj
Field of Study	Chemistry
Thesis Advisor	Professor Dr. ORAWON CHAILAPAKUL
Thesis Co Advisor	Professor Dr. TIRAYUT VILAIVAN

Accepted by the FACULTY OF SCIENCE, Chulalongkorn University in Partial Fulfillment of the Requirement for the Master of Science

.... Dean of the FACULTY OF SCIENCE

(Professor Dr. POLKIT SANGVANICH)

THESIS COMMITTEE

.... Chairman

(Associate Professor Dr. VUDHICHAI PARASUK)

.... Thesis Advisor

(Professor Dr. ORAWON CHAILAPAKUL)

.... Thesis Co-Advisor

(Professor Dr. TIRAYUT VILAIVAN)

.... Examiner

(Associate Professor Dr. NARONG PRAPHAIRAKSIT)

.... Examiner

(Associate Professor Dr. NATTAYA NGAMROJANAVANICH)

.... External Examiner

(Assistant Professor Dr. Amara Apilux)

สริดา เนาว์รุ่งโรจน์ : การพัฒนาตัวรับรู้เชิงสีฐานกระดาษสำหรับการตรวจวัดดีเอ็นเอของ
เชื้อไวรัสฮิวแมนแพพิลโลมา. (DEVELOPMENT OF PAPER-BASED COLORIMETRIC
SENSOR FOR DETERMINATION OF HUMAN PAPILLOMAVIRUS DNA) อ.ที่ปรึกษา
หลัก : ศ. ดร.อรวรรณ ชัยลภากุล, อ.ที่ปรึกษาร่วม : ศ. ดร.ธีรยุทธ วิไลวัลย์

งานวิจัยนี้เป็นการพัฒนาอุปกรณ์ฐานกระดาษร่วมกับเทคนิคตรวจวัดเชิงสีโดยใช้พิโรลิดิ
นิลเพป์ไทด์นิวคลีอิคแอซิดเป็นสารทางชีวภาพสำหรับการตรวจวัดดีเอ็นเอของเชื้อไวรัสฮิวแมน
แพพิลโลมา โดยมีการนำอนุภาคทองคำขนาดนาโนที่ทำให้เสถียรด้วยโมเลกุลเดกซ์ตรินมาใช้
สำหรับเป็นสารให้สี และด้วยคุณสมบัติที่โดดเด่นของพิโรลิดินิลเพป์ไทด์นิวคลีอิคแอซิดเหนี่ยวนำให้
อนุภาคทองคำขนาดนาโนเกิดการรวมตัวกัน ส่งผลให้เกิดการเปลี่ยนแปลงสีของสารละลาย โดย
การเข้าคู่กันระหว่างพิโรลิดินิลเพป์ไทด์นิวคลีอิคแอซิดและดีเอ็นเอเป้าหมาย โมเลกุลของพิโรลิดินิล
เพป์ไทด์นิวคลีอิคแอซิดส่วนที่เหลือจากการเข้าคู่จะไปเหนี่ยวนำให้อนุภาคทองคำขนาดนาโนเกิด
การรวมตัวกัน ทำให้เกิดการเปลี่ยนแปลงสีที่สามารถตรวจวัดได้ การเปลี่ยนแปลงสีที่แตกต่างกันไป
นั้นสัมพันธ์กับปริมาณของดีเอ็นเอเป้าหมาย ซึ่งสามารถวิเคราะห์ความเข้มสีที่เปลี่ยนแปลงไปด้วย
แอปพลิเคชั่นวัดความเข้มสีโดยใช้สมาร์ทโฟน ภายใต้สภาวะที่เหมาะสมได้ช่วงความสัมพันธ์
ระหว่างค่าความเข้มสีที่เปลี่ยนแปลงไปและความเข้มข้นของดีเอ็นเอของเชื้อไวรัสฮิวแมนแพพิล
โลมาเป็นเส้นตรงในช่วง 1-1000 นาโนโมลาร์ โดยที่ค่าสัมประสิทธิ์สหสัมพันธ์อยู่ที่ 0.9996 และขีด
จำกัดต่ำสุดของการตรวจ วัดอยู่ที่ 1 นาโนโมลาร์ จากการทดลอง นอกจากนี้พิโรลิดินิลเพป์ไทด์นิว
คลีอิคแอซิดแสดงถึงความจำเพาะต่อดีเอ็นเอของเชื้อไวรัสฮิวแมนแพพิลโลมาที่เหนือกว่าดีเอ็นเอที่
มีลำดับเบสผิดไป 1 ตำแหน่ง, 2 ตำแหน่ง และดีเอ็นเอที่มีลำดับเบสไม่ตรงกับดีเอ็นเอเป้าหมาย อีก
ทั้งตัวรับรู้เชิงสีฐานกระดาษสำหรับการตรวจวัดดีเอ็นเอที่พัฒนาขึ้นเป็นอุปกรณ์ที่ใช้งานง่าย มีความ
ว่องไว และจำเพาะกับเอ็นเอของเชื้อไวรัสฮิวแมนแพพิลโลมา ดังนั้นตัวรับรู้ดีเอ็นเอนี้สามารถเป็น
หนึ่งในตัวเลือกสำหรับตรวจคัดกรองเชื้อไวรัสฮิวแมนแพพิลโลมา ซึ่งเป็นสาเหตุหลักที่ก่อให้เกิด
โรคมะเร็งปากมดลูกได้

สาขาวิชา	เคมี	ลายมือชื่อนิสิต ....
ปีการศึกษา	2562	ลายมือชื่อ อ.ที่ปรึกษาหลัก ....
		ลายมือชื่อ อ.ที่ปรึกษาร่วม ....

6172142023 : MAJOR CHEMISTRY

KEYWORD:

Sarida Naorungroj : DEVELOPMENT OF PAPER-BASED COLORIMETRIC SENSOR FOR DETERMINATION OF HUMAN PAPILLOMAVIRUS DNA. Advisor: Prof. Dr. ORAWON CHAILAPAKUL Co-advisor: Prof. Dr. TIRAYUT VILAIVAN

In this work, a paper-based analytical device (PAD) based on colorimetric assay using pyrrolidinyl peptide nucleic acid (acpcPNA) probe was developed as a sensor for the detection of Human papillomavirus (HPV) DNA. Dextrin-stabilized gold nanoparticles (d-AuNPs) was employed as a colorimetric reagent. The aggregation of d-AuNPs can be induced by positively charged acpcPNA generating a distinctive color change. After the hybridization of acpcPNA and DNA target, the residual acpcPNA probe can cause different degrees of the d-AuNPs aggregation, resulting in the detectable color change. The different color change before and after the introduction of the DNA target as a function of DNA concentration was quantified by analyzing the color intensity through a smartphone application. Under the optimal conditions, the linearity in the range from 1 to 1000 nM with a correlation coefficient of 0.9996 and an experimental limit of detection of 1 nM was obtained. In addition, the acpcPNA probe exhibited high selectivity for the target DNA over single-base-mismatch, two-base-mismatch, and non-complementary DNA. The proposed smartphone-based colorimetric DNA sensor offers a simple, sensitive, and selective platform for detecting HPV DNA. Therefore, this DNA sensing device can be utilized as an alternative tool for point-of-care and economical screening of HPV that is a major cause of cervical cancer.

Field of Study:	Chemistry	Student's Signature ....
Academic Year:	2019	Advisor's Signature ....
		Co-advisor's Signature ....

ACKNOWLEDGEMENTS

TABLE OF CONTENTS

จุฬาลงกรณ์มหาวิทยาลัย
CHULALONGKORN UNIVERSITY

LIST OF TABLES

LIST OF FIGURES

LIST OF ABREVIATIONS

d-AuNPs	Dextrin-stabilized gold nanoparticles
HPV	Human papillomavirus
DNA	Deoxyribonucleic acid
PNA	Peptide nucleic acid
PADs	Paper-based analytical devices
TEM	TEM
LOD	Limit of detection
mg	milligram
g	gram
μL	microliter
mL	milliliter
L	liter
μM	micromolar
nM	nanomolar
°C	degree celsius

CHAPTER I

INTRODUCTION

1.1 Introduction

Cervical cancer is considered a sexually infected disease which tends to increase annually. It is currently classified as the second most common type of cancer in women after breast cancer [1]. The main cause of cervical cancer is Human papillomavirus (HPV) which can be sexually transmitted leading to changes in genital areas such as vagina, cervix, penis, and anus [2]. There are more than 100 types of HPV that can be found in humans. However, they can be categorized into two types including high-risk and low-risk species. HPV type 16 (HPV-16) is one of the high-risk species which is the most commonly found in humans more than the others [2, 3]. Therefore, screening of HPV, especially HPV type 16 at the early stage of infection is extremely important to avoid the formation of cancer and also prevent the onset of the disease. A traditional screening method for HPV infections in clinical diagnostic is the pap-smear test [4], which still has some drawbacks such as time-consuming, low sensitivity and provided a moderate false-negative result [5]. Nowadays, DNA diagnosis such as polymerase chain reaction (PCR) with generic primers and digene hybrid capture assay (HC2) [6-8] has become an alternative method for HPV monitoring since it offers higher accuracy and sensitivity than the traditional pap-smear test. However, this method relies on the costly and complicated of the standard commercial instruments and trained personnel which make it unsuitable for HPV screening in limited resources set-ups and terms of point-of-care testing (POCT).

To date, Paper-based analytical devices (PADs) become a great attractive technology for developing miniaturized devices because of its versatility, portability, inexpensiveness, ease of use and small reagent volume requirement. With these advantages, PADs have received great

attention and been found in various fields, especially in chemical [9], biological analysis [10] and also applied in POCT application [11, 12]. Various analytical techniques including colorimetry [13], fluorometry [14] and electrochemistry [15] have been most frequently combined with PADs. Among these methods, colorimetry is particularly attractive for several fields due to their simplicity, absence of complicated instruments and ability to perform semi-quantitative results [16].

Gold nanoparticles (AuNPs) have received considerable attention to use as a colorimetric agent based on their unique properties such as stability, high extinction coefficients, strong size-dependent optical properties [17, 18]. In addition, with a non-toxicity and biocompatibility properties that exhibited the AuNPs appropriate with the biological applications [19, 20]. The color changes of AuNPs that can be easily visualized by the naked eye depending on the important factors such as their environment, shape, size, physical dimension and morphology [21]. Moreover, AuNPs also provided good compatibility with simple and sensitive DNA detection that performs a major role in the field of clinical diagnostics [22], food analysis [23], and environmental monitoring [24].

In recent years, Peptide nucleic acid (PNA) has been an attractive probe for DNA detection. PNA, a synthetic oligonucleotide mimetic having an uncharged peptide-like backbone, was firstly introduced by Nielsen and co-workers in 1991 [25]. The negatively charged DNA favorably binds with the neutral PNA followed Watson-Crick base-pairing rules [26] without the electrostatic repulsion as observed in the DNA-DNA binding. The outstanding characteristics of PNA including high thermal stability, greater sequence specificity and mismatch discrimination sensitivity, and less salt-dependency make PNA become an interesting alternative probe for DNA detection. Among PNA variants being investigated thus far, Vilaivan's group have been developed a new conformationally constrained pyrrolidinyl PNA system with an α,β-peptide backbone of D-prolyl-2-aminocyclopentane carboxylic acid called acpcPNA [27]. The acpcPNA has recently emerged as an efficient probe for DNA detection for biological application [28-30] to improve the selectivity and

specificity of the analysis due to it offers a stronger affinity and higher sequence specificity in binding to DNA when compared to the original Nielsen's PNA.

In order to develop a rapid and simple method for HPV DNA determination, the paper-based analytical device combined with colorimetric detection using AuNPs as a colorimetric agent and the acpcPNA as a probe for DNA detection was developed. As the benefits of this research including simple fabrication and operation, rapid response, high sensitivity, and selectivity, this proposed system can be utilized as an alternative tool for qualitative and semi-quantitative of HPV DNA in a biological sample which still has few studies on this area.

1.2 Objectives of the research

The objectives of this research are divided into two parts as follows:

1. To develop a paper-based colorimetric DNA sensor for determination of human papillomavirus.

2. To apply the proposed sensor for screening of human papillomavirus DNA in biological samples.

1.3 Scope of this research

The paper-based sensor for detecting HPV DNA using colorimetric assay based on acpcPNA induced AuNPs aggregation was introduced. In order to investigate HPV DNA detection, the numerous processes were carried out. Firstly, the preliminary reaction of AuNPs aggregation by the acpcPNA with and without DNA complementary (HPV DNA) was studied. The color change of AuNPs was observed and the color intensity of the solution was analyzed by application on a smartphone to differentiate the color intensity. For the data confirmation, the Transmission

electron microscopy (TEM) was operated to study the size and morphology of the AuNPs. In addition, Ultraviolet-visible (UV-Vis) spectroscopy was also used for studying the color changing of AuNPs. Designing and fabrication of the paper-based sensor were investigated using adobe illustrator software and wax printing technique, respectively. To obtain the optimal condition of HPV DNA determination, all experimental conditions consisted of the type of gold nanoparticle stabilizer, the ratio of gold nanoparticle and phosphate buffer solution, the volume and concentration of acpcPNA probe and incubation time were optimized. For analytical performance, the different concentrations of HPV DNA were measured to identify the linear relationship against the color intensity signal. In addition, the limit of detection was also calculated. To investigate the selectivity of the proposed method, complementary DNA, single-base mismatch, two-base mismatch and non-complementary DNAs were tested under the same experimental conditions. Moreover, the storage stability of the proposed sensor was also studied under room temperature (25 ℃) and 4 ℃. Finally, the proposed sensor was applied to test with biological samples.

CHAPTER II

THEORY AND LITERATURE REVIEWS

2.1 Human papillomavirus (HPV)

In 1996, the World Health Organization recognized Human papillomavirus (HPV) as the main cause of cervical cancer in women. HPV is one of the most common causes of sexually transmitted infection. Recently, more than 100 types of HPV can be found in human, and approximately 40 types infect the genital area such as vagina, cervix, penis, and anus. Genital HPV types are mainly classified into 2 groups: high-risk and low-risk HPV types according to their association with cervical cancer (Table 2.1). Although low-risk HPV types are less likely to cause cervical cancer than high-risk HPV types, they can develop as genital warts and other diseases. However, HPV type 16 is the most common type that can be found in human more than other high-risk types [31]. In 2018, there was an estimated number of 311,000 reported cases who died from HPV cancer, moreover, 85% of these cases were reported from developing countries [32, 33]. The major cause of high mortality rate is due to a lack of access to diagnostic and treatment. Therefore, the screening of HPV at the early stage of infection is extremely important to avoid the development of cancer and prevent the onset of the disease.

Table 2.1 HPV types group based on their association with cervical cancer.

High-risk HPV types	Low-risk HPV types
16, 18, 31, 33, 34, 35, 39, 45, 51, 52, 56, 58, 59, 68, 69, 70, 73, 82	6, 11, 40, 42, 43, 44, 53, 54, 61, 70, 72, 81, 89

The traditional clinical method for HPV diagnosis is pap-smear test or pap test [5]. This method collects specimens directly from the cervix using a sample collected equipment such as

brush or spatula and then placed directly on a glass slide and fixed with a chemical fixative to analyze cell morphology. The aim of the pap test is to identify the abnormal cells which show a tendency for cervical cancer. However, the pap smear test still has some limitations. Only 8% of the samples collected from the cervix can be used for analysis and the cells are not distributed uniformly on the glass slide resulting in false-negative results (approximately 30%). In addition, the contamination compounds such as blood and mucosa presented in the collected samples can interfere cell morphology interpretation under light microscopic observation. From these reasons, the pap test provides low accuracy and sensitivity for HPV diagnosis [5].

Recently, HPV DNA detection has become an alternative method for HPV diagnosis. The two techniques most widely used for HPV DNA detection are polymerase chain reaction (PCR) with generic primers and hybrid capture version 2 (HC2) [5]. The PCR is a relatively simple technique for amplification of DNA sequences. The main components of the PCR reaction consist of target DNA, DNA polymerase, deoxynucleotide triphosphates (dNTPs), oligonucleotide primers and reaction buffer. The amplification method of the PCR showed in Figure 2.1. Firstly, the denaturation of the double-stranded DNA is performed using disintegration of the hydrogen bonds between complementary bases of duplex DNA as a result of two single-stranded DNA molecules. After that, each of the single-stranded DNA templates are annealed by the primers. Then, the primer-template is adhered with DNA polymerase for hybridizing and generating DNA formation. Herein, the specificity and efficiency of the hybridization depends on the annealing temperature. The free dNTPs are added to generate complementary base to the template in the 5'-3' direction (elongation step). A single cycle of the PCR amplification consists of denaturation, annealing and elongation step. After the completion of the amplification assay, both of the original template strands and synthesized strands are developed to template strands for the further cycle, resulting in exponential DNA target amplification [34]. The HC2 technique is a DNA

qualitative assay based on a nucleic acid hybridization with signal amplification using microplate chemiluminescence (Figure 2.2). The detection is based on the selective binding between HPV DNA-RNA duplex and captured antibody coated on surface of microplate. The secondary antibody conjugated with alkaline phosphatase is then added to the system and caused the chemiluminescent signal relating to HPV DNA concentration. These two assays are appropriate for high-throughput detection. The DNA-based methods exhibit higher accuracy, selectivity and sensitivity than the pap test because these methods use the specific probes to bind with genetic DNA target of detecting virus according to those mentioned above. However, they still have some drawbacks. For the PCR with generic primers method, the sensitivity and specificity of this method depend on many factors, for example, there is more than one primer sequence in a DNA molecule that used for each analysis causing the wrong sequences on the DNA copy molecule. Another case is the longer length of the target DNA sequence leading to the wrong sequence of the copied target obtained. For the HC2 method, the major disadvantage of this method is ineffective differentiation of the HPV types within the groups. Moreover, these two methods need the costly and complicated instrument, and highly trained personnel which make them unsuitable for HPV screening in limited resources set-ups and personnel.
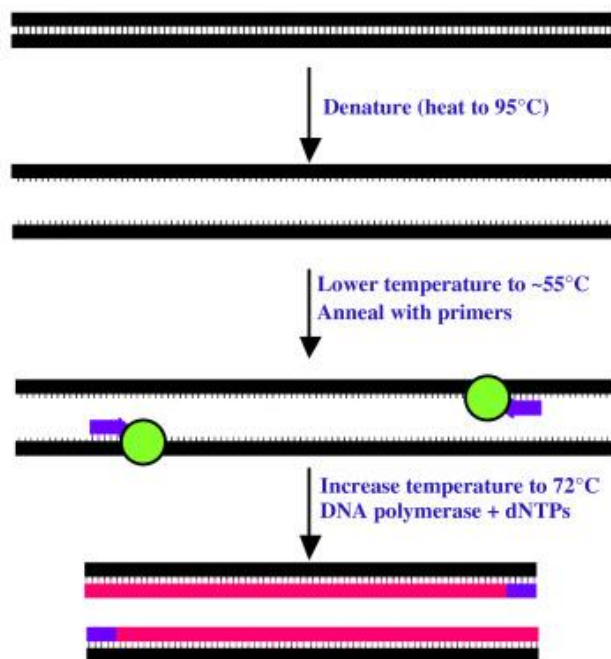
Figure 2.1 The PCR amplification steps including denaturation, annealing and elongation step [34]
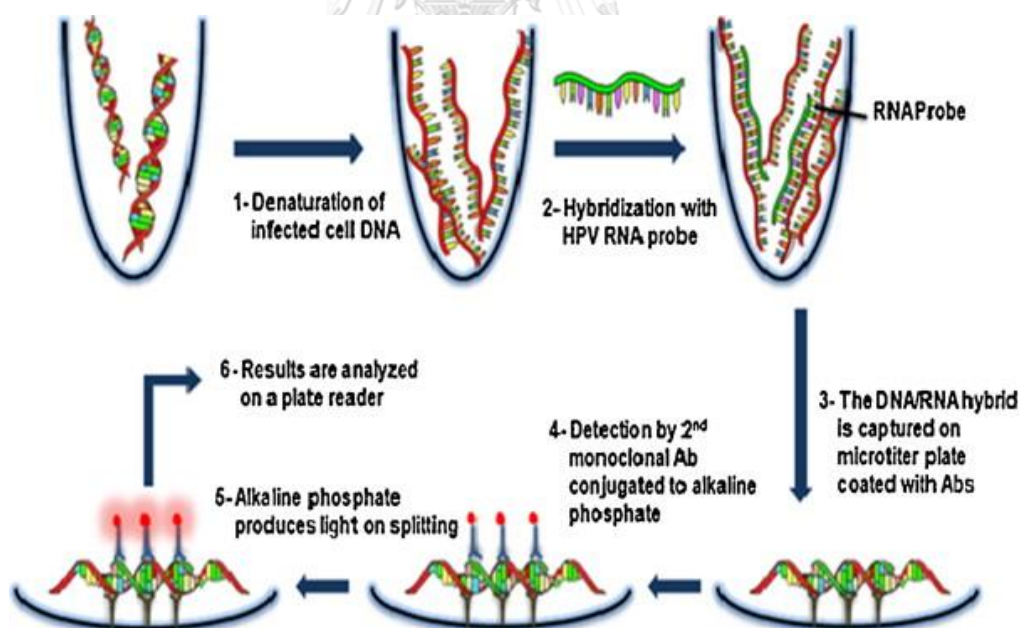
Figure 2.2 Schemetic of HC2 method for the HPV DNA detection [35]

2.2 Paper-based analytical device (PADs)

Paper-based analytical device (PADs) is an analytical tool using paper as a material for making miniaturized devices. PADs were firstly introduced by Whiteside group in 2007 [36]. PADs have been broadly utilized for analysis in several applications such as chemical, biological, medical and environmental fields due to their various advantages including small samples volume and reagents requirement, fast analysis time, portability, disposability and inexpensiveness. Moreover, PADs also provide affordable and user-friendly analytical chemistry tool that is appropriate for on-site detection and point-of-care (POC) testing [37]. Recently, several methods have been proposed for PADs fabrication to create hydrophobic barrier that can confine the direction or area of aqueous solution (Figure 2.3), including (A) photolithography [38], (B) inkjet printing [39], (C) plasma treatment [40], (D) wax printing [41], (E) screen printing [42], and (F) laser treatment [43]. Among these methods, the wax-printing method is the most widely used due to its easy fabrication and suitability for mass production.
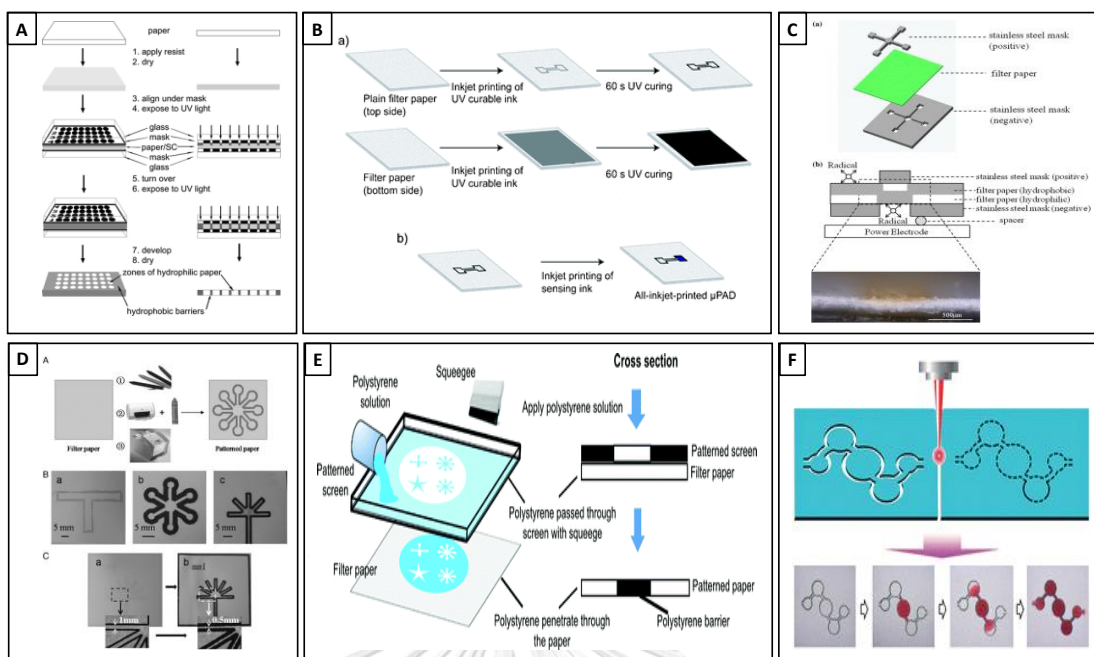
Figure 2.3 Fabrication methods for creating PADs; (A) photolithography [38], (B) inkjet printing [39], (C) plasma treatment [40], (D) wax printing [41], (E) screen printing [42], and (F) laser treatment [43].

2.3 Colorimetry

Colorimetric assay has been a great attractive method [44-47] owing to their advantages including simple operation, rapid response, and adaptable for semi-quantitative analysis. Colorimetric method is classified as an optical detection, meaning identification of the analyte species by observing the visible change of color by the reaction between colorimetric agent and target analyte. In addition, color intensity can be quantified as the amount of the target analyte. A well-known colorimetric method is a Litmus paper used as a pH indicator for testing of acidic or basic condition of the solution. Under acidic condition, the blue litmus paper turns to red whereas the red litmus paper turns to blue under basic condition. The color change relates to the concentration of the acidic or basic compound in the sample which can be simply monitored by naked eyes. To increase the sensitivity of the measurement, several instruments such as spectrophotometer or colorimeter were introduced for improving capability of this

method. Recently, portable devices. for example, camera or smartphone became more popular and widespread coupled with colorimetric method due to their interesting properties such as portability, ease of use, uncomplicatedness and inexpensive instrument. Several applications i.e. ImageJ, Color Assist, RGB Colormeter and Adobe photoshop have been available on smartphone which can be used for analyzing the color intensity of the reaction. Benefitting from these advantages (simple operation, low cost, and no complicated apparatus needed), the colorimetric method has been applied in various fields and in biological application, especially clinical and point-of-care diagnosis.

2.3.1 Nanomaterials

Nanoparticles are usually defined as a particle with size dimensions approximately in the range of 1-100 nm. The outstanding properties of nanoparticles including high surface-to-volume ratio, size- and distance-dependent optical properties make the nanoparticles broadly utilized as a colorimetric agent for colorimetric detection in different fields such as chemical [48], environmental [49] and especially in biological [50-52] applications. Several nanoparticles including gold nanoparticles, silver nanoparticles, magnetic nanoparticles, and semiconductor nanoparticle (Quantum dots, QDs) have been used as a colorimetric agent for biological applications. Among them, gold nanoparticles (AuNPs) are one of the good candidates which commonly used owing to their stability, biocompatibility, and high extinction coefficients. The color change of AuNPs is based on localized surface plasmon resonance (LSPR) phenomenon which occurred by a strong interparticle plasmon coupling and an associated perturbation in the LSPR band of two particles which are in close proximity, resulted in a red-shifting. A visible color change of the solution can be verified by changing of the morphology, nanoparticle size and interparticle distance [53]. A brief illustration is shown in Figure. 2.4.
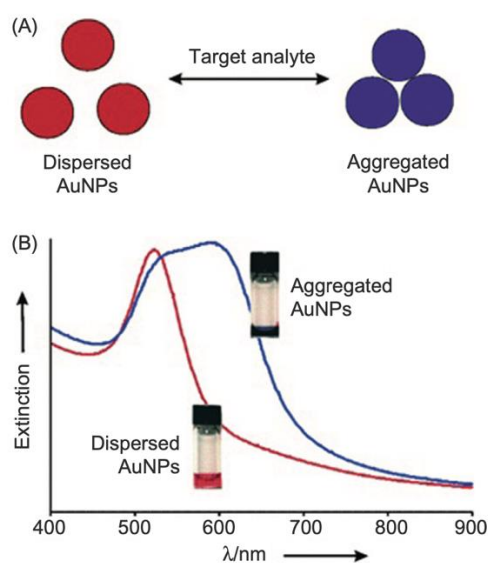
Figure 2.4 (A) The LSPR-based colorimetric assay based on AuNPs dispersion and aggregation. (B) Surface plasmon absorption bands of AuNPs in dispersion (red) and aggregation (blue) form [54]

2.3.2 Nanoparticle stabilizers

Although AuNPs have been utilized in several biological application [55-57], they still have some limitations such as unstable under high-ionic salt condition resulted in AuNPs aggregation [58]. To solve this problem, many researches have been demonstrated about functionalization of AuNPs to increase the stability of AuNPs and prevent the salt-induced aggregation in biological condition. Generally, AuNPs are synthesized and functionalized with organic molecules to increase the stability and provide modifiable functional groups for conjugation chemical reaction such as citrate molecules which is the most common functionalized molecules used in recent years for AuNPs stabilization. The citrate-stabilized AuNPs provides the uniform particle sizes and good stability in aqueous solution. Even though, it can be used for functionalization of AuNPs, it cannot prevent salt-induced aggregation. Moreover, AuNPs synthesized in organic molecules or functionalized by non-biocompatible molecules are not suitable for biological applications because of their toxicity [59]. Several recent researches have introduced green synthetic

methodology to synthesize and stabilize AuNPs. Carbohydrate compounds have received great attention for being an AuNPs stabilizer with biofriendly properties. They contain a lot of hydroxyl and carbonyl groups which provide sugar-stabilized nanoparticle with excellent H-bonding abilities in a supramolecular structure. This stabilization of carbohydrate-capped AuNPs is called a macromolecular crowding which impact many molecular and physical processes. This carbohydrate-stabilized AuNPs methods exhibit several outstanding advantages for example the synthesis of AuNPs was proceeded under biofriendly conditions, the water-soluble and non-toxic compounds were utilized for the synthesis process which was generated in only one-step [60].

2.4 DNA detection

Deoxyribonucleic acid or DNA is an important biomolecule because it encodes genetic information capacity of life. DNA was discovered long ago before Watson-Crick can explain their structures as double helix [26]. DNA is made up of nucleotide monomers. Each monomer units comprise of three-components: a five-carbon sugar (deoxyribose), a phosphate group, and a nitrogenous base. There are four types of the nitrogenous bases which are adenine (A), thymine (T), guanine (G), and cytosine (C). The DNA detection is based on the specific binding between the DNA target and its complementary probe following Watson-Crick rules. The nucleotide chain is formed by binding between sugar and phosphate group of neighbor molecules resulting in a phosphate backbone. The nitrogenous bases of two polynucleotide chains are hybridized via H-bonds, following base pairing rules (C with G and A with T) [61]. The DNA binding performs in an anti-parallel orientation which means that the 5' end of one strand pairs with the 3' end of its complementary strand as shown in Figure 2.5. With the advantages of the high specificity of the binding between the base sequence on the DNA duplex, DNA detection has become an

alternative method for several fields such as biological analysis [62], clinical analysis[63], and forensic

science [64].
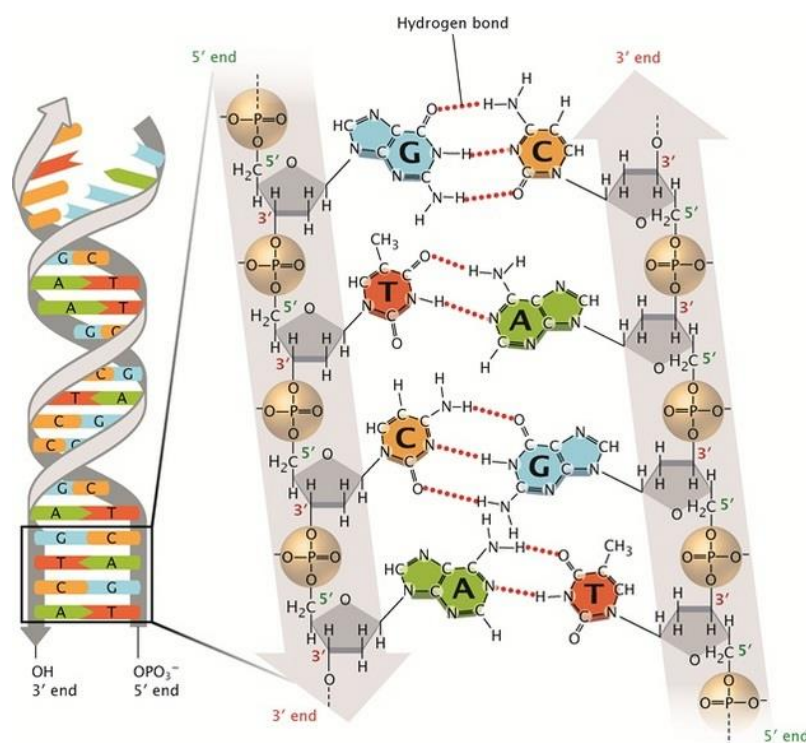
Figure 2.5 Base pairing in DNA [61]

2.5 Peptide nucleic acid (PNA)

The important key parameter affecting the detection performance is probe selection. The

selection of a suitable probe can enhance the performance of the detection. In 1991, Nielsen

and co-workers firstly presented a synthetic DNA mimics containing an uncharged peptide-like

backbone called peptide nucleic acid (PNA) [25]. The backbone of PNA is structurally

homomorphous with the deoxyribose backbone and compose of N-(2-aminoethyl) glycine units

to which the nucleobases (purine and pyrimidine) are bound via a methyl carbonyl linker (Figure

2.6, left) [65, 66]. PNA is depicted as peptides, with the N-terminus at the left (or at the top) position

and the c-terminus at the right (or at the bottom) position. The formation of PNA-DNA duplexes

follows Watson–Crick base-pairing rules though hydrogen bonds (Figure 2.6, right). The hybridization of PNA-DNA duplexes is stronger and more stable comparing with DNA-DNA duplexes because of the absence of electrostatic repulsion on the backbone [66]. In addition, PNA also exhibits the outstanding characteristics for example high thermal stability, less salt-dependency, excellent sequence specificity and mismatch discrimination sensitivity [67]. Because of several favorable characteristics of PNA, it becomes an interesting alternative probe for DNA biosensors application instead of the original DNA probe. However, the original PNA can bind to complementary DNA in both parallel and antiparallel orientation. The hybridization in parallel orientation is not included in Watson–Crick base-pairing rules giving non-selective hybridization that provides less selectivity of detection.
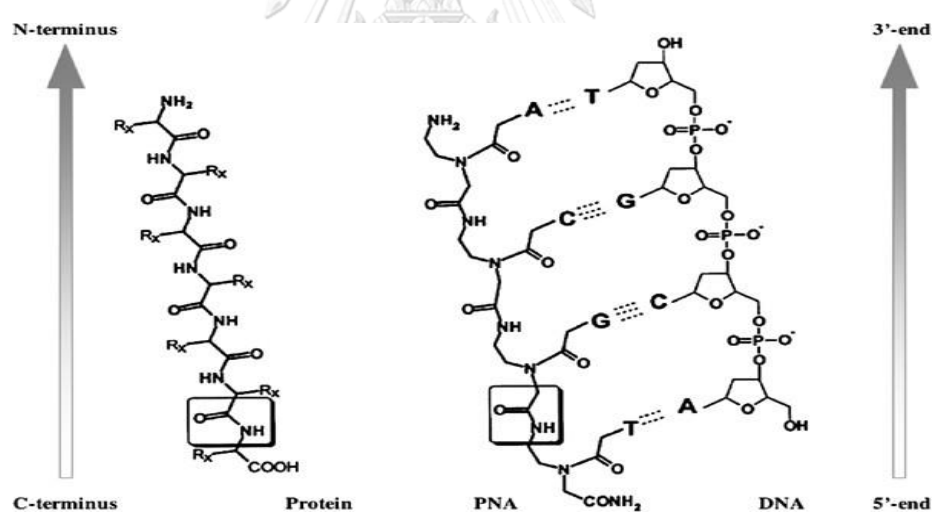
Figure 2.6 Chemical structures of PNA (left) and the hybridization between PNA-DNA duplexes according to the Watson–Crick rules (right) [66]

In recent years, several kinds of PNA probes have been successfully developed as shown in Figure 2.7. A new conformationally constrained pyrrolidinyl PNA system with a nonchimeric α/β-dipeptide backbone derived from nucleobase-modified proline and cyclic β-amino acids

was introduced by Vilaivan's group [27]. The binding efficiency of DNA, RNA, and self-pairing depends on the conformation consisting of the pyrrolidine ring and the β-amino acid on the PNA backbone. Pyrrolidinyl PNA containing a (2′R,4′R)-proline/ (1S,2S)-2-aminocyclopentanecarboxylic backbone (acpcPNA) (Figure 2.8) exhibits sequence specificity and high binding affinity to DNA over RNA. In addition, the acpcPNA conformation also provides the binding between PNA and DNA in antiparallel orientation corresponding to Watson-Crick rules with a low tendency for self-hybridization. The acpcPNA offers several advantages over the original Nielsen's PNA including higher sequence specificity and stronger affinity for binding to DNA target. Due to several favorable characteristics of the acpcPNA, it has been widely applied as a probe in the DNA sensing and biological applications [28-30].
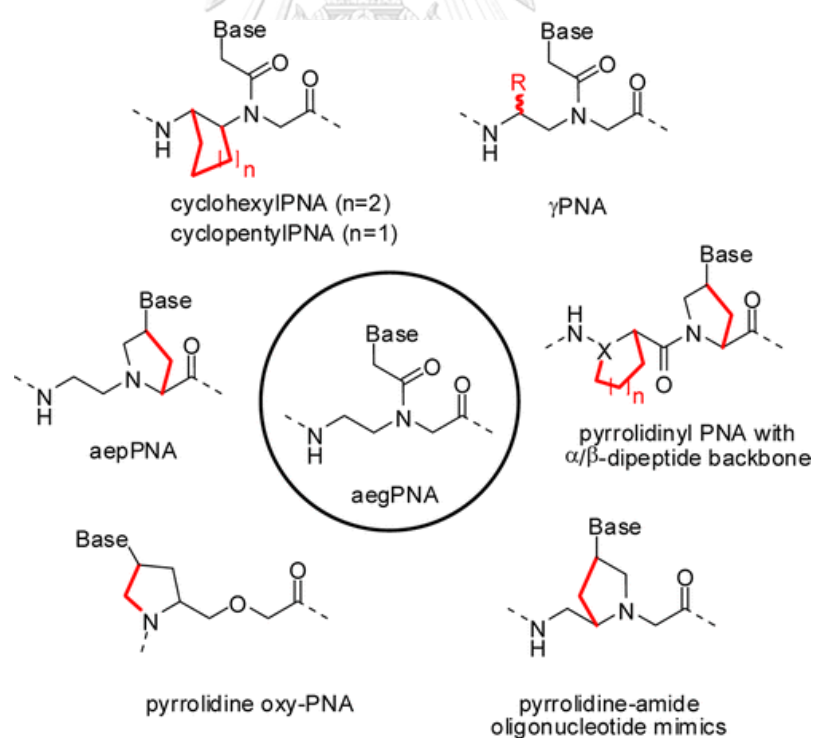
Figure 2.7 Several kind of conformationally constrained PNA analogues [27]
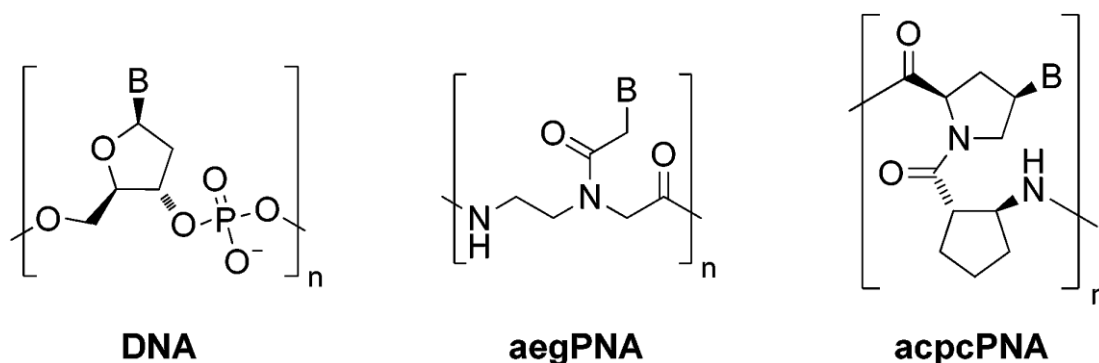
Figure 2.8 Structure of DNA, original Nielsen's PNA and Vilaivan's acpcPNA probe [29]

2.6 Literature reviews

Human papillomavirus (HPV) is a main threatening virus disease which can cause the cervical cancer through the sexually transmitted infection in human. Among 100 HPV types, only 18 genital HPV types are considered to cause the risky cancer, especially, types 16 which is the most found in human [31]. The traditional clinical method for HPV screening is Pap-smear test [5]. This technique still has some disadvantages such as low accuracy and sensitivity for HPV diagnosis, and also requires extensively trained and experienced technicians for data analysis. DNA-based diagnosis including PCR with generic primers and Hybrid Capture version 2 (HC2) [5] has been demonstrated as an alternative technique for HPV screening with high accuracy, selectivity and sensitivity, and high-throughput testing. Nevertheless, these DNA-based methods still have some limitations such as specific conditions requirement, ineffective in distinguishing HPV types. Moreover, the standard commercial instrument of DNA testing is costly, relatively complex and relies on skilled personnel which are not appropriate for point-of-care testing (POCT).

To overcome these limitations of the common clinical techniques, various analytical methods have been demonstrated for HPV DNA detection.

In 2014, Jampasa and coworkers [68] reported electrochemical biosensor for HPV type 16 DNA detection using acpcPNA as a probe. The acpcPNA probe was covalently attached with

anthraquinone (AQ) which is a redox-active label on the N-terminus and was immobilized onto a carbon-based screen-printed electrode. The electrochemical signal response can be achieved from AQ molecule. The linear range of this work was found in the range of 0.02-12.0 μM with a limit of detection and quantitation of 4 and 14 nM, respectively.

In 2017, Jimenez and coworkers [69] proposed a DNA biosensor based on gold-coated nanoparticles-modified superparamagnetic nanomaghemite (AuMNPs) for E6 HPV-16 DNA detection. The surface of AuNPs was modified with oligo-deoxyribonucleotides probe of E6 HPV-16 DNA. After hybridization of HPV-16 DNA target and its probe, conjugation of QDs to antibodies was recognized onto the binding of viral ssDNA which can be detect fluorescence signal. The linearity of the PCR-amplified HPV DNA sample was in the range of 0.05-200 μM with detection limit at 100 pM.

Paper-based analytical devices (PADs) become an attractive technology for making miniaturized device because of its versatility, portability, disposability, inexpensiveness, ease of use, suitability for on-site screening. and adaptability for point-of-care testing (POCT). Colorimetric method has received great attention for combining with PADs because of the simple operation, relative ease of data acquisition and interpretation. Gold nanoparticles (AuNPs) have gained considerable attention in using as colorimetric agents owing to their advantages of direct observation of color change by naked eyes, high stability and biocompatibility. Recently, paper-based colorimetric sensors based on AuNPs have been widely used for various applications, especially in biological application.

In 2015, Choleva and co-workers [70] presented a paper-based sensor using gold nanoparticles as colorimetric agent for determination of antioxidant activity in food samples. Gold ions were immobilized onto the paper surface. In the presence of antioxidant compounds, gold ions were reduced to AuNPs and color turn from white or yellow to red. The color change can be

visualized by naked eyes or imaging devices for example cameras or camera-based smartphones. For the real sample application, Gallic acid was selected to investigate the performance of the proposed sensors. The proposed sensors provided a linearity in the range of 10 μM–1.0 mM, with detection limits at the low and ultra-low μM levels (i.e. <1.0 μM). Moreover, the proposed sensor has been verified for the determination of antioxidant activity in food and drink samples and the results correlated well with the standard detection methods. This method exhibits several benefits including high sensitivity, simplicity, rapid responsiveness, portability, and well correlated results with standard methods.

In 2020, Aydindogan and co-workers [71] introduced a paper-based colorimetric immunosensor to detect cancer biomarkers including alpha-fetoprotein (AFP) and mucin-16 (MUC16) utilizing smartphone. AuNPs were used as a bioconjugates for signal production tool. To fabricate a spot-like point-of-care (POC) immunoassay, AuNPs conjugated with cysteamine (AuNP-Cys) were immobilized on the nitrocellulose (NC) membrane and then antibodies were conjugated to the nanoparticle on the detection pad. In the presence of AFP or MUC16, the visible color change occurred which images were taken by using a smartphone and measured via image and color analysis software (Image J). The linear range of AFP and MUC16 were found in the range of 0.1-100 ng/mL and 0.1-10 ng/mL, respectively. Limit of detection (LOD) was found to be 1.054 ng/mL for AFP and 0.413 ng/mL for MUC16.

Although AuNPs were widely used in biological applications with their unique properties, but the limitations in high salt concentrations (high ionic strength condition) leading to less stability and aggregation of AuNPs also presented. Many researches have demonstrated a method for increasing the stability of AuNPs and resisting salt-induced aggregation to overcome these limitations.

In 2004, Katti and co-workers [60] reported a one-step general methodology for the synthesis of carbohydrate-stabilized AuNPs. Four categories of carbohydrates such as monosaccharide (glucose), disaccharide (sucrose, maltose, lactose), trisaccharide (raffinose), and polysaccharide (starch) were chosen for investigating the stabilized properties. The size and particle size distribution of AuNPs directly depends on the sugar stabilizer. The smaller size (a diameter of 3 nm) of AuNPs occurred in a lactose whereas the larger size (a diameter of 39 nm) appeared in a starch matrix. In addition, the AuNPs stabilities toward aggregation also depends on carbohydrate molecules. The results showed that glucose-stabilized AuNPs provided the least stability. In contrast, other carbohydrates provided the stability more than 5 hours. In the case of starch-stabilized AuNPs exhibited outstanding stability owing to the core structure of starch molecules contains H-bonding which are capable of folding around the nanoparticles and expected to prevent the AuNPs aggregation.

In 2010, Wang and co-workers [59] introduced a green synthesis of dextran-stabilized AuNPs. Dextran function as a stabilizer and a reducing agent which provided well dispersed, homogenous, and biocompatible AuNPs. In order to compare the dextran-capped AuNPs with citrate-capped AuNPs from the previous reports, the toxicity and the ability of preventing aggregation in high ionic conditions were also investigated. The toxicological results showed that dextran-stabilized AuNPs showed excellent biocompatibility similar to citrate-stabilized AuNPs. However, the resistance towards high ionic strength-induced aggregation capability of citrate-capped AuNP was poor when compared to dextran-capped AuNPs. Under high ionic conditions, the aggregation of citrate-stabilized AuNPs occurred resulting in the color turned from red to blue whereas the dextran-stabilized AuNPs still remained as the red color (Figure 2.9). The results indicated that the dextran-stabilized AuNPs showed a good biocompatibility without toxicity and

provided a high stability to prevent aggregation in high ionic conditions that can be applied for biological assay.
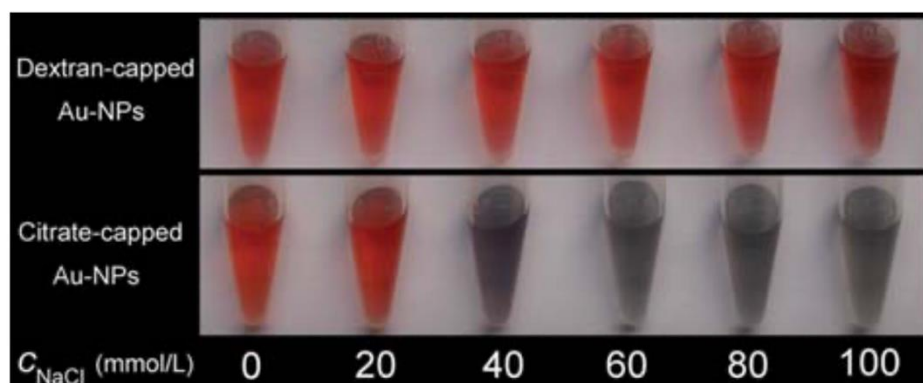
Figure 2.9 Investigations of dextran- and citrate-stabilized AuNPs preventing salt-induced aggregation

The biocompatibility and non-toxicity properties of AuNPs make them suitable for biological applications. DNA detection has been greatly attractive as a utility for biosensor application due to its outstanding advantages such as good selectivity with the target analytes.

In 2018, Baetsen-Young and co-workers [58] developed a dextrin-stabilized AuNPs (d-AuNPs) for unamplified genomic DNA (gDNA) nanosensor. The d-AuNPs were stable in a salt conditions but they showed dispersion and aggregation behavior for sequence-specific detection. In the presence of gDNA target, the target reactions were stabilized via the formation of a single stranded DNA probe (ssDNAp) and target gDNA complex. The results indicated a proposed mechanism whereby genomic ssDNA secondary structure formation during ssDNAp-to-target gDNA binding enables d-AuNPs stabilization in high salt conditions. This method successfully detected extracted pathogen DNA with the linear range of 2.9 aM - 29 fM and detection limit as low as

2.94 fM. In addition, the results of crude DNA from pathogen matrix provided a linearity in range of 0.026 fM - 0.016 fM for P. cubensis DNA.

In 2019, Liu and co-workers [72] proposed a visual colorimetric assay for DNA detection using AuNPs based on different electrostatic properties of single strand DNA (ssDNA) and double strand DNA (dsDNA). The negatively charged phosphate backbone of ssDNA exhibited easy binding with AuNPs and preventing salt-induced aggregation of AuNPs. On the other hand, the dsDNA exhibited aggregation of AuNPs because of the disturbance of the adsorption between dsDNA and AuNPs. When the target DNA existed in the system, the hybridization between target DNA and ssDNA probe occurred. After that and ascorbic and chloroauric acid were added to the mixed solution, and the color of the solution turned from red to purple in 10 min.

One of the key components is the probe that can determine a specificity of the target analytes for detection. Short oligodeoxynucleotide probes have been recently employed in conventional DNA biosensors. However, in recent years, several alternative probes have been successfully used with great potential. To date, a pyrrolidinyl PNA system with an α,β-peptide backbone of D-prolyl-2-aminocyclopentane carboxylic acid , called acpcPNA which was introduced by Vilaivan's group [27] has been used as a probe for DNA analysis. The acpcPNA offers several advantages over conventional DNA or the original Nielsen's PNA probes including stronger affinity and higher sequence binding specificity. Moreover, it also hybridizes with DNA target in only an antiparallel orientation with a low self-hybridization. Therefore, the acpcPNA has been extensively applied as a probe in DNA detection to improve the selectivity and specificity of the analysis.

In 2009, Kanjanawarut and coworkers [73] developed colorimetric DNA detection based on unmodified metallic nanoparticle aggregation. A neutral-charged PNA probe was used for inducing particle aggregation. The hybridization of PNA–DNA duplex occurred in the presence of

complementary DNA, the particles remained stable because of the negative charge repulsions of the DNA strands in the complexes. On the other hand, in the absence of a complementary DNA, the aggregation of particle occurred since the free PNA molecules removed the charge repulsion. The color change in UV–vis adsorption spectra can be rapidly observed. The mixture of AgNPs and AuNPs was validated with a shorter and a longer PNA sequences. The proposed method can detect the target DNA in the presence of at least 10 times of interference DNA. The two-component nanoparticle provided a high selectivity for single-base-mismatch DNA.

In 2009, Su and co-workers [74] demonstrated mixed-based PNA oligomers inducing citrate-coated AuNPs and AgNPs which can be interrupted by duplex of target DNA and PNA. The results showed that PNA and PNA–DNA duplexes bind to AuNPs and AgNPs and modulate stability differently relative to their DNA duplexes as followed: (1) The mix-based PNA inducing immediate particle aggregation deepened on concentration and chain-length of PNA; (2) The PNA provided a higher affinity to AuNPs and AgNPs than ssDNA; (3) Although PNA–DNA duplexes exhibited a stable double helix structure similar to dsDNA, they had capability for preventing salt-induced aggregation; and (4) AuNPs and AgNPs showed the same all the characteristics. However, AgNPs is more sensitive in response which is suitable for colorimetric assays.

In 2013, Laopa and co-workers [28] proposed a colorimetric paper-based device utilizing acpcPNA as a probe for specific DNA sequences detection. The filter paper was modified with grafted polymer brushes of quaternized poly(dimethylamino)ethyl methacrylate (QPDMAEMA) to generate a positively charged on the surface. Then, a DNA target was first immobilized via electrostatic interactions between the negative charges of the phosphate backbone of DNA and positive charges of the QPDMAEMA brushes. The immobilized DNA provided a yellow product generated by a horseradish peroxidase (HRP)-labeled streptavidin from the enzymatic reaction

which can be observed by naked eyes. The proposed method provided high specificity for the complementary DNA over single-base-mismatch DNA with limit of detection at 10 fmol.

In 2015, Jirakittiwut and co-workers [29] reported cellulose-based DNA sensor utilizing acpcPNA as a probe for DNA detection. The acpcPNA probe was immobilized onto cellulose paper by covalently attaching. After DNA incubation, cationic organic dyes could be applied for observing the binding between target DNA and acpcPNA probe via electrostatic interaction between the positively charged dye and the negatively charged DNA. By combining the relatively inexpensive cellulose paper, and the performance of acpcPNA probe, the proposed DNA sensor platform could have potential as an economical point-of-care DNA testing device.

In 2017, Teengam and co-workers [75] developed a paper-based colorimetric assay for DNA detection based on acpcPNA-induced silver nanoparticles (AgNPs) aggregation for screening of infected disease including Middle East respiratory syndrome coronavirus (MERS-CoV), Mycobacterium tuberculosis (MTB), and HPV. The acpcPNA carrying positively charged lysine at the C-terminus was designed as a probe to induce the aggregation of citrate-stabilized AgNPs. In the presence of target DNA, the AgNPs remain stable because of the sufficient charge repulsion of the anionic acpcPNA-DNA duplexes. Therefore, the hybridized and unhybridized acpcPNA probe interact differently with the AgNPs resulting in color change, which could be observed both in the solution and on the paper. The detection limits of this method were 1.53, 1.27, and 1.03 nM for MERS-CoV, MTB and HPV DNAs, respectively.

In 2020, Jirakittiwut and co-workers [76] presented paper-based sensor for detection of Hemoglobin E (HbE) single-point mutation in thalassemia genes. The paper was immobilized with epi-acpcPNA probe via an amide bond. DNA target was extracted by PCR employing biotin-tagged DNA. After the hybridization between biotinylated target DNA and acpcPNA probe, the visualized dark blue color can be observed via alkaline phosphatase-linked streptavidin. The proposed

sensor demonstrated good discrimination among different genotypes from validation of 100 human blood samples. Therefore, the proposed DNA sensing platform has potential to be an alternative tool for thalassemia diagnosis in primary cares.

In order to develop a simple, portable, fast analysis time, sensitive and selective DNA sensor for screening of HPV, a paper-based analytical device based on acpcPNA induced d-AuNPs aggregation for colorimetric determination utilizing smartphone as a readout device will be introduced for screening of HPV DNA in biological samples.

CHAPTER III

EXPERIMENT

This chapter provides the information of chemicals used for synthesis of d-AuNPs and all preparation of standard solutions. The operation instruments used in this work are also described.

3.1 Instruments and apparatus

The instruments which used in all experiments are listed in Table 3.1.

Table 3.1 List of instruments and apparatus

Instruments and apparatus	Suppliers
Analytical balance, Mettler Toledo	Mettler, Switzerland
Hot air oven	Memmert, USA
Hotplate stirrer, C MAG HS 7	IKA, Germany
iphone 6s	Apple, USA
Microcentrifuge tubes	Axygen scientific, USA
Micropipette	Eppendorf, Germany
Milli-Q water system (18 MΩ cm^{-1})	Millipore, Bedford, USA
Matrix-assisted laser desorption ionization time-of-flight (MALDI-TOF) mass spectrometer, Microflex series	Bruker Daltonik GmbH, Germany
pH meter	Metrohm, Switzerland
Reverse-phase (C18 column) high performance liquid chromatography (HPLC) on a Water Delta 600^{TM} system	GenTech Scientific, USA

Instruments and apparatus	Suppliers
Smartphone gadget	EOSCE, Thailand
Universal pipette tips	Plusmed, Thailand
Volumetric flask and other glassware	SCHOTT, Germany
Vortex mixer	Scientific industries, United states
Wax printer, ColorQube 8570	Fuji Xerox, Japan

3.2 Chemicals and reagents

All chemicals and reagents used in this work are listed in Table 3.2. The sequences of synthetic DNA oligonucleotides are shown in Table 3.3

Table 3.2 List of chemicals and reagents

Chemicals	Suppliers
acpcPNA probe	Organic Synthesis Research Unit, Thailand
Dextrin (from corn) ($C_6H_{12}O_6$)	Sigma-Aldrich, USA
Magnesium Chloride ($MgCl_2$)	Merck, Germany
Phosphate buffered saline (PBS) tablet pH 7.4	Sigma-Aldrich, USA
Potassium tetrachloroaurate (III) ($KAuCl_4$)	Wako, Japan
Sodium carbonate (Na_2CO_3)	Merck, Germany
Sodium Chloride (NaCl)	Carlo-Erba, Italy
Synthetic DNA oligonucleotides	Pacific science, Thailand
Whatman chromatography paper No.1	Sigma-Aldrich, USA

Table 3.3 List of synthetic DNA oligonucleotides used in this study

Synthetic DNA oligonucleotides	Sequences (5'→3')
Complementary HPV DNA type 16	GCTGGAGGTGTATG
Single-base mismatch DNA	GCTGGACGTGTATG
Two-base mismatch DNA	GCTGGACGTGTGTG
Non-complementary DNA	GGATGCTGCACCGG

* Red color letters represented base mismatch sequence in complementary HPV DNA type 16.

3.3 Chemicals and reagents preparation

3.3.1 Preparation of 20 mM KAuCl$_4$

The 0.0378 g of KAuCl$_4$ (MW = 377.88 g/mol) was weighed and dissolved in Milli-Q water. Then, the solution was adjusted the volume to 5 mL.

3.3.2 Preparation of 25 g/L of dextrin solution

The 0.5380 g of dextrin from corn powder was weighed and dissolved in Milli-Q water. Then, the solution was adjusted the volume to 5 mL.

3.3.3 Preparation of 10 %w/v Na$_2$CO$_3$

The 0.50 g of Na$_2$CO$_3$ (MW = 105.98 g/mol) was weighed and dissolved in Milli-Q water. Then, the solution was adjusted the volume to 5 mL.

3.3.4 Preparation of 0.01 M PBS

One tablet of PBS was dissolved in 200 mL of Milli-Q water and stored at 4 °C.

3.3.5 Preparation of NaCl stock and working solutions

A stock solution of 1 M of NaCl was prepared in Milli-Q water by weighing 0.0597 g of NaCl (MW = 58.44 g/mol), then dissolving in Milli-Q water and adjusting volume to 1 mL. The working NaCl solution was prepared by diluting stock solution to various concentrations at 50, 60, 70, 80, 90 and 100 mM.

3.3.6 Preparation of $MgCl_2$ stock and working solutions

A stock solution of 1 M of $MgCl_2$ was prepared in Milli-Q water by weighing 0.0962 g of $MgCl_2$ (MW = 95.21 g/mol), then dissolving in Milli-Q water and adjusting volume to 1 mL. The working $MgCl_2$ solution was prepared by diluting stock solution to various concentrations at 50, 60, 70, 80, 90, 100, 120, 150, 200, 250 and 300 mM.

3.3.7 Preparation of acpcPNA working solutions

The working acpcPNA solutions were prepared by diluting 250 μL of stock solution to various concentrations at 1, 2, 5, 10, 25 and 50 μM in 0.01 PBS buffer at pH 7.4.

3.3.8 Preparation of DNA oligonucleotides working solutions

The working DNA oligonucleotides solutions were prepared by diluting 250 μL stock solution to various concentrations at 1, 50, 100, 250, 500, 750, 1000, 2000, 5000, 7500, 10000 and 25000 nM in 0.01 PBS buffer at pH 7.4.

3.3.9 Preparation of one-based, two-based mismatch DNA and non-complementary DNA solution

The one-based, two-based mismatch DNA and non-complementary DNA solution were prepared by diluting 200 μL of each stock solution to concentrations at 5000 nM in 0.01 PBS buffer at pH 7.4.

3.4 Synthesis of dextrin-stabilized gold nanoparticles

Dextrin-stabilized gold nanoparticles were synthesized using the Baetsen-Young's method [58]. Briefly, 5 mL of 20 mM $KAuCl_4$ and 20 mL of 25 g/L of dextrin solution were mixed. Then, 10% sodium carbonate (Na_2CO_3) was added to the mixture to adjust the pH of the solution to 9.0 and the final volume was adjusted to 50 mL with Milli-Q water. Finally, the particle formation reaction was allowed to proceed at 50 °C in the dark for 8 hours.

3.5 Synthesis of acpcPNA probe for HPV type 16

The acpcPNA probe for HPV type 16 with a base sequence of CATACACCTCCAGC-LysNH$_2$ (written in the N$\longrightarrow$C direction) was obtained from Organic synthesis Research Unit. The acpcPNA probe was synthesized by standard Fmoc solid-phase peptide synthesis method as previously described [77]. Briefly, The PNA was synthesized on a Tentagel resin equipped with a Rink amide linker. A positively charged lysinamide group was attached at the C-terminus of acpcPNA probe sequence to exhibit inducing nanoparticle aggregation property. After the complete reaction process, the nucleobase protecting groups of the PNA was removed by 1:1 (v/v) aqueous ammonia: dioxane at 60 °C overnight and cleaved from the solid support with trifluoroacetic acid (TFA). Finally, the acpcPNA were purified by reverse-phase HPLC using C18 column with 0.1% (v/v) trifuoroacetic acid (TFA) in H_2O-MeOH gradient and the purity was confirmed to be more than 90%. The identification of the synthetic acpcPNA probe was confirmed by MALDI-TOF MS analysis on a Microflex MALDI-TOF mass spectrometer (Bruker Daltonics).

3.6 Fabrication of paper-based colorimetric DNA sensors

In this work, the wax-printing method was used to fabricate PADs. Figure 3.1 shows the design of patterned paper which was created using Adobe illustrator software. The detection zone and control zone were designed in a circular shape with 0.5 cm diameter and surrounded by waxed barrier with hydrophobic property (blue part). Next, the wax pattern was printed onto Whatman No. 1 filter paper using a wax printer (Xerox ColorQube 8570). Then, the patterned paper was incubated at 150 °C for 30 sec in a hot air oven. After that, a piece of transparent tape was attached on the backside of the paper to prevent the leakage from the bottom. Finally, the acpcPNA probe solution was dropped onto the detection zone prior to use as a paper-based colorimetric DNA sensor.
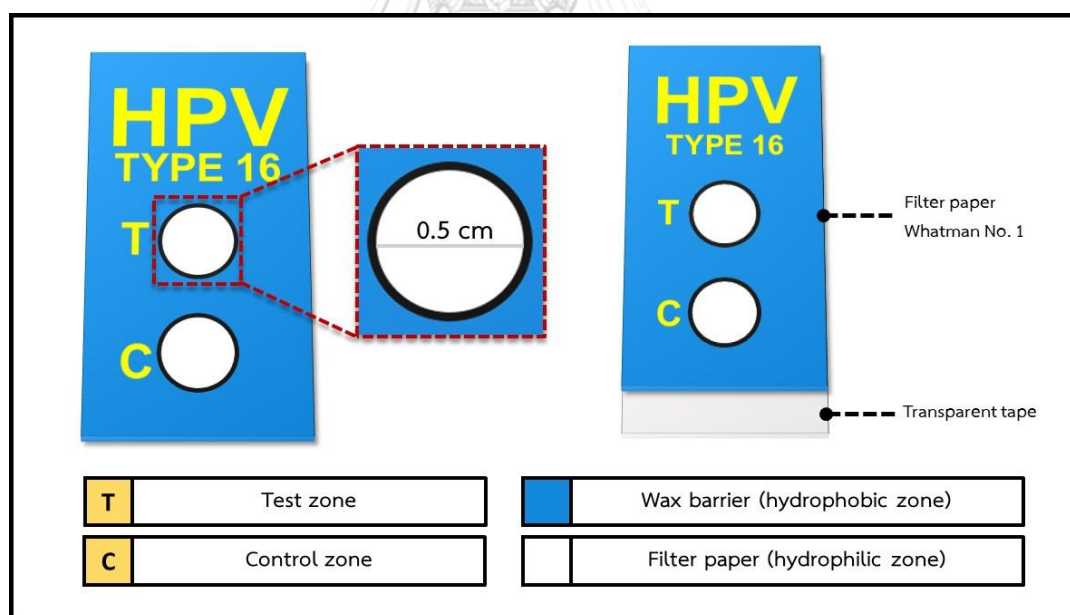
Figure 3.1 Design of paper-based colorimetric DNA sensors

3.7 Colorimetric detection of HPV DNA target on PADs

For colorimetric detection, 10 **µ**L of the d-AuNPs and 1 **µ**L of DNA target were mixed. Then, the mixture was dropped onto the detection zone and adjusted the volume to 15 **µ**L using 0.01 M PBS buffer at pH 7.4. After that, the mixture solution of the d-AuNPs (10 **µ**L) and 0.01 M PBS buffer at pH 7.4. (5 **µ**L) was dropped onto the control zone. Finally, the AuNPs aggregation occurred within 30 min and the color change can be observed by naked eyes. The image of color change was recorded via smartphone coupled with camera gadget (Figure 3.2A) for light controlling and then imported to RGB Colorimeter application for IOS developed by White Marten UG for analyzing color intensity of the solution using red channel (Figure 3.2B)
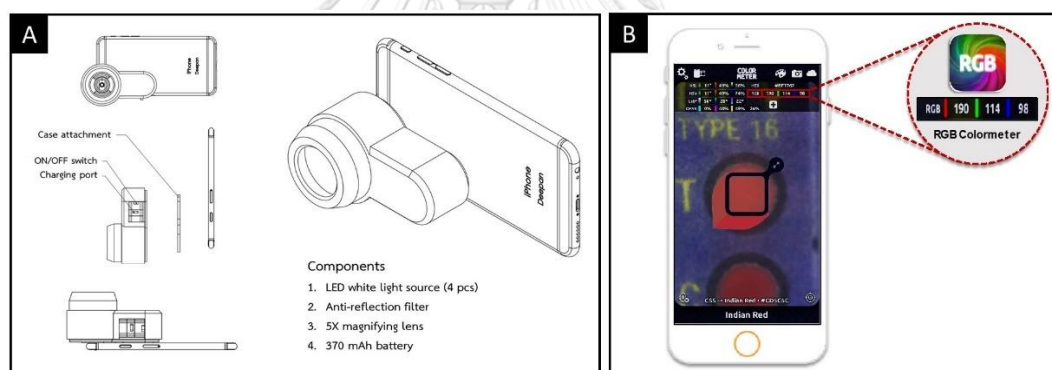
Figure 3.2 (A) Structure of the camera gadget coupled with smartphone readout device and its components (B) Image of color intensity analyzing by using RGB Colorimeter application

3.8 UV-vis spectroscopy characterization

UV-vis spectroscopic technique was used for verifying the color change of the AuNPs solution. 0.01 M PBS buffer at pH 7.4 was used as a blank solution to measure absorbance at wavelengths ranging from 200 to 800 nm. Then, the absorbance of d-AuNPs solution at various conditions as shown in Table 3.3 was measured.

Table 3.3 List of d-AuNPs conditions for UV-vis spectroscopy

No.	Conditions
1	d-AuNPs
2	d-AuNPs + acpcPNA probe
3	d-AuNPs + complementary DNA
4	d-AuNPs + acpcPNA probe + complementary DNA

3.9 Optimization of the experimental conditions I

3.9.1 Effect of PBS buffer ratio

The salt in the PBS buffer which was used for the acpcPNA probe and DNA sample preparation steps can have a pronounced effect on the AuNPs stability. Moreover, biological samples also generally contain biological salts such as NaCl. Therefore, the effect of the PBS ratio on AuNPs aggregation was studied. The conditions ratio of d-AuNPs:PBS were showed in Table 3.4. The mixed solution in each condition was dropped on to PADs for measuring color intensity.

Table 3.4 List of d-AuNPs:PBS conditions

Ratio (10:x)	d-AuNPs (μL)	PBS (μL)	Milli-Q water (μL)
0	10	0	10
1	10	1	9
2	10	2	8
3	10	3	7
4	10	4	6
5	10	5	5
6	10	6	4

3.9.2 Effect of PBS buffer mixing time

To investigate the mixing time of the d-AuNPs and PBS which can affect the d-AuNPs aggregation, the mixed solution of the d-AuNPs and PBS in the ratio of 10:4 was studied with the time ranging from 0 to 40 min.

3.9.3 acpcPNA probe concentration

The acpcPNA probe concentrations were optimized to achieve suitable acpcPNA probe concentration for the highest differential color intensity (Δ intensity) obtained before and after addition of acpcPNA probe (Δ intensity = Intensity $_{d-AuNPs}$ − Intensity $_{d-AuNPs + acpcPNA}$). Various concentration of acpcPNA probe ranging from 1 to 50 μM in PBS buffer at pH 7.4 was investigated. All experiments were performed using 10 μL of d-AuNPs and 1 μL of 2 μM DNA target.

3.9.4 Incubation time

To examine the suitable reaction time, the incubation time ranging from 0 to 40 min were optimized. In this parameter, the Δ intensity obtained before and after addition of the target DNA (Δ intensity = Intensity $_{with target DNA}$ − Intensity $_{without target DNA}$). All experiments were done using 10 μL of d-AuNPs, 3 μL of 50 μM acpcPNA probe and 3 μL of 1 μM DNA target.

3.10 Salt-induced d-AuNPs for interfering stability of d-AuNPs study

The interfering stability of d-AuNPs was demonstrated in order to minimize the acpcPNA probe concentration. The salt compounds including NaCl and $MgCl_2$ were selected to investigate the destabilizing effects of d-AuNPs. The d-AuNPs was tested with 1 μL of NaCl concentration in the range of 0 to 100 mM and 1 μL of $MgCl_2$ concentration in the range of 0 to 300 mM.

3.11 Optimization of the experimental conditions II

3.11.1 MgCl$_2$ and acpcPNA probe concentration

To investigate the MgCl$_2$ and acpcPNA probe concentration that provided the highest signal respond, 1 μL of MgCl$_2$ concentration in the range of 100-300 mM was further optimized with 2 μL of acpcPNA probe concentration in the range of 1-10 μM. In this parameter, the Δ intensity obtained before and after addition of 1 μM target DNA in the mixed solution of d-AuNPs and MgCl$_2$ (Δ intensity = Intensity $_{\text{with target DNA}}$ − Intensity $_{\text{without target DNA}}$).

3.11.2 Incubation time

To demonstrate the complete reaction time, incubation time ranging from 0 to 40 min were optimized. All experiments were done using 10 μL of d-AuNPs, 1 μL of 100 mM MgCl$_2$, 2 μL of 2 μM acpcPNA probe and 2 μL of 1 μM DNA target.

3.12 Analytical performance I and II

The calibration curve was obtained by plotting the relationship between the different DNA concentrations and the Δ intensity obtained before and after addition of target DNA (Δ intensity = Intensity $_{\text{with DNA target}}$ − Intensity $_{\text{blank}}$) as x and y axis, respectively. The error bars represent one standard deviation (SD) obtained from three independent measurements (n=3). After that, the R^2 or correlation coefficient was calculated.

3.13 Selectivity study

For selectivity study, the measurement of 50 nM DNA complementary was compared with different kinds of DNA, including single-based mismatch DNA, two-based mismatch DNA and non-

complementary DNA at a concentration of 5000 nM. The Δ intensity was obtained from three independent measurements (n=3).

3.14 Stability study

To demonstrate the stability, the proposed sensors were kept at room temperature (25 °C) as well as the refrigerator at 4 °C prior to use. The HPV DNA at concentration of 50 nM was selected as a target DNA for monitoring the efficiency of the sensor after 7 days of the storage.

3.15 Real sample analysis

To demonstrate the applicability of the proposed sensor for the detection of HPV DNA in real biological samples, the DNAs from cell lines including SiHa (positive-cell line), CaSki and C33A (negative-cell line) were detected. the DNAs from cell lines were obtained from the Human Genetics Research Group, Chulalongkorn University. The DNA samples preparation method followed the previously described procedure [30]. In addition, a serial dilution concentration of SiHa (positive-cell line) was also evaluated to determine the concentration-dependent signal response.

CHAPTER IV

RESULTS AND DISCUSSION

This chapter describes the results and discussion of colorimetric detection based on acpcPNA-induced AuNPs aggregation concept, optimization conditions. Furthermore, the analytical performances, selectivity study, storage stability study and real sample application are also described.

4.1 Colorimetric detection of HPV DNA based on acpcPNA-induced AuNPs aggregation

The mechanism of acpcPNA-induced AuNPs aggregation in the presence of complementary DNA and non-complementary DNA is shown in Figure 4.1. Dextrin-stabilized AuNPs (d-AuNPs) was obtained in a well dispersed form due to the steric effect and electrostatic repulsion [59, 78]. In the presence of DNA target, the AuNPs were still dispersed since the negative charges on the DNA strand that do not affect the aggregation of d-AuNPs. The aggregation of the d-AuNPs occurred when the acpcPNA probe was added, resulting in a distinctive color change from red to purple owing to the electrostatic interaction between the negative charges of d-AuNPs and positive charges of the acpcPNA probe deriving from the lysine at C-terminus. When both the acpcPNA probe and the target DNA were present, a specific hybridization between the acpcPNA probe and DNA target occurred via base pairing. Therefore, no color change was observed due to the depletion of the acpcPNA probe that can induce the AuNPs aggregation and the color of the solution remained red. When the amounts of the DNA target was limit, the acpcPNA probe remained from the pairing with the DNA can induce the d-AuNPs aggregation leading to some color change. The color change is related to the concentration of the target DNA. In contrast,

when non-complementary DNA was present, the acpcPNA probe cannot hybridize and remained

in the free form that can induce the aggregation of the d-AuNPs.
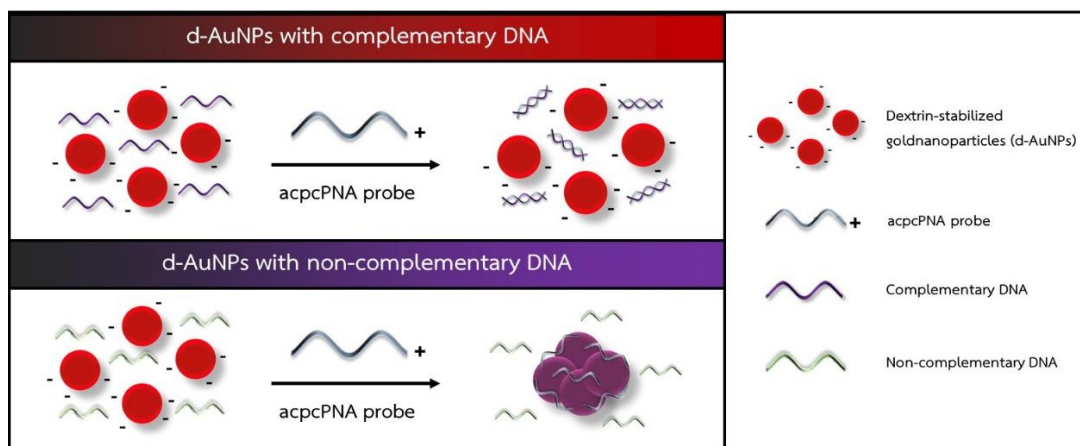
Figure 4.1 The proposed mechanism for colorimetric detection of HPV DNA based on acpcPNA-

induced d-AuNPs aggregation in the presence of complementary DNA and non-complementary

DNA

The concept of this work was demonstrated as shown in Table 4.1. The color of d-AuNPs

remained red after adding only complementary DNA. In contrast, when the acpcPNA probe was

added to the d-AuNPs solution, the color turned to purple due to the aggregation of d-AuNPs.

However, in the presence of the complementary DNA, the hybridization of DNA and acpcPNA

probe occurred and the color remained red due to the depletion of free acpcPNA probe that can

induce d-AuNPs aggregation. The color change from red to purple related to the DNA

concentration in the system.

Table 4.1 List of d-AuNPs conditions and their photograph

d-AuNPs in various conditions	Photograph
d-AuNPs	
d-AuNPs + complementary DNA	
d-AuNPs + acpcPNA probe	
d-AuNPs + acpcPNA probe + complementary DNA	

In addition, the color intensity of the d-AuNPs solution in each condition was also verified. The image of the solution was taken via a smartphone coupled with a camera gadget for light control. Then, the image was imported to the RGB Colorimeter application for measuring the color intensity. To interpret the results, the intensity in the red channel was used to quantitate the "redness" of the reaction. When the solution is red which means containing a high amount of red value resulting in high color intensity. On the other hand, when the solution turns to another color, such as purple, it means the amount of red value is decreased, leading to a decrease of color intensity in the red channel.

Figure 4.2 showed the color intensity of the d-AuNPs solution for each condition. The d-AuNPs contained the complementary DNA (d-AuNPs +DNA) provide the same intensity as d-AuNPs in the red channel indicating that the aggregation process is not affected by the negatively charged DNA. On the other hand, the aggregation of d-AuNPs occurred since the electrostatic repulsion is shielded when the acpcPNA probe was introduced into the d-AuNPs solution (d-AuNPs+acpcPNA). The color of the solution changed to purple, thus resulting in decreasing of color intensity in the red channel. When the complementary DNA was added into the mixture of

d-AuNPs and acpcPNA probe, the solution is still in red color. The color intensity of the solution (d-AuNPs+acpcPNA+DNA) increased with the increasing of complementary DNA (d-AuNPs+acpcPNA). The hybridization of the target DNA with the acpcPNA probe minimized the aggregation of the d-AuNPs induced by the acpcPNA probe.
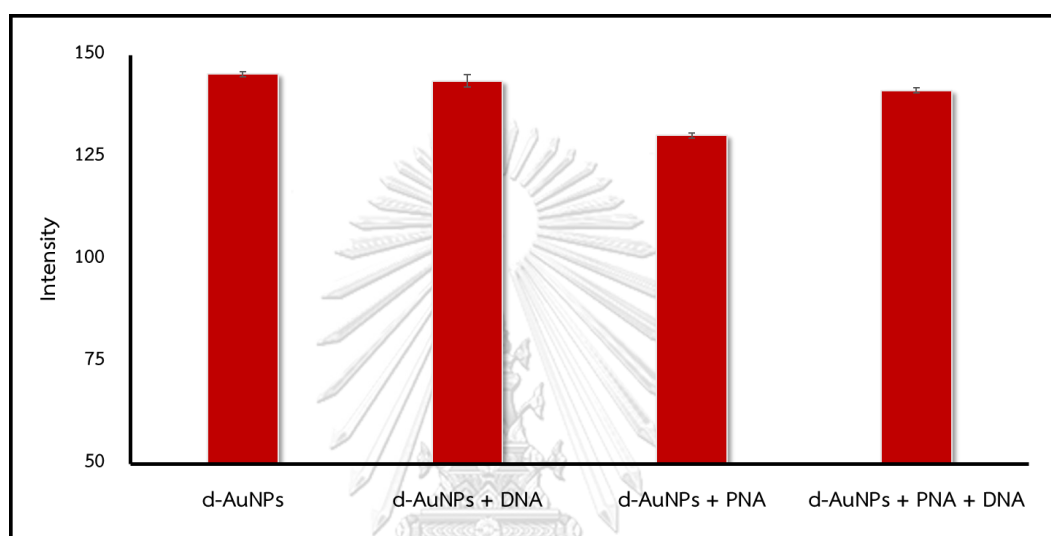
Figure 4.2 Color intensity of d-AuNPs in various condition measuring by RGB Colorimeter application in red channel

In addition, the comparison of the intensity in the red, green, and blue channels was also studied. It was found that the red channel provided the most obvious difference in color intensities under each condition compared to other channels. The highest sensitivity from the red channel is unexpected due to the reaction involves the change in red color (Figure 4.3). Therefore, measuring color intensity in the red channel was chosen for further experiments.
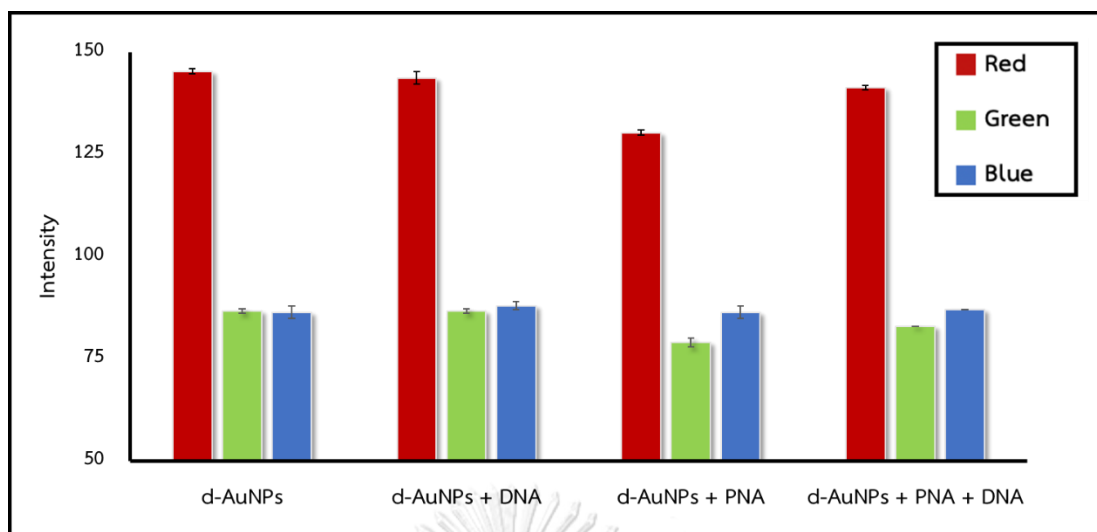
Figure 4.3 Color intensity of d-AuNPs in various condition measuring by RGB Colorimeter

application in red, green and blue channel

4.2 Characterization of acpcPNA-induced d-AuNPs aggregation

To confirm the performance of the acpcPNA-induced d-AuNPs aggregation, d-AuNPs under various conditions were characterized. Firstly, the color change of d-AuNPs which related to the d-AuNPs aggregation was characterized by UV-vis absorption spectrophotometry. Figure 4.4 shows the UV-vis absorption spectra of d-AuNPs under various conditions. The solution of d-AuNPs (red line) provides an absorption peak at 522 nm which was in good agreement with the previous work [58]. After adding complementary DNA (blue line), the peak at 522 nm which was similar to the peak of d-AuNPs was still present. This indicated that the complementary DNA did not affect the d-AuNPs aggregation. In contrast, when the acpcPNA probe was added (purple line), the solution turned to purple and the peak slightly shifted to 552 nm (red shift) due to the aggregation of d-AuNPs. In the presence of the acpcPNA probe and its complementary DNA in d-AuNPs solution, a red solution and a slight red shifting of the absorption peak (at 526 nm) were also observed. This result indicated that some acpcPNA probe hybridized with the

complementary DNA, leading to lower amounts of the acpcPNA probe that can induce the d-AuNPs aggregation, resulting in both dispersion form and aggregation forms of the d-AuNPs.
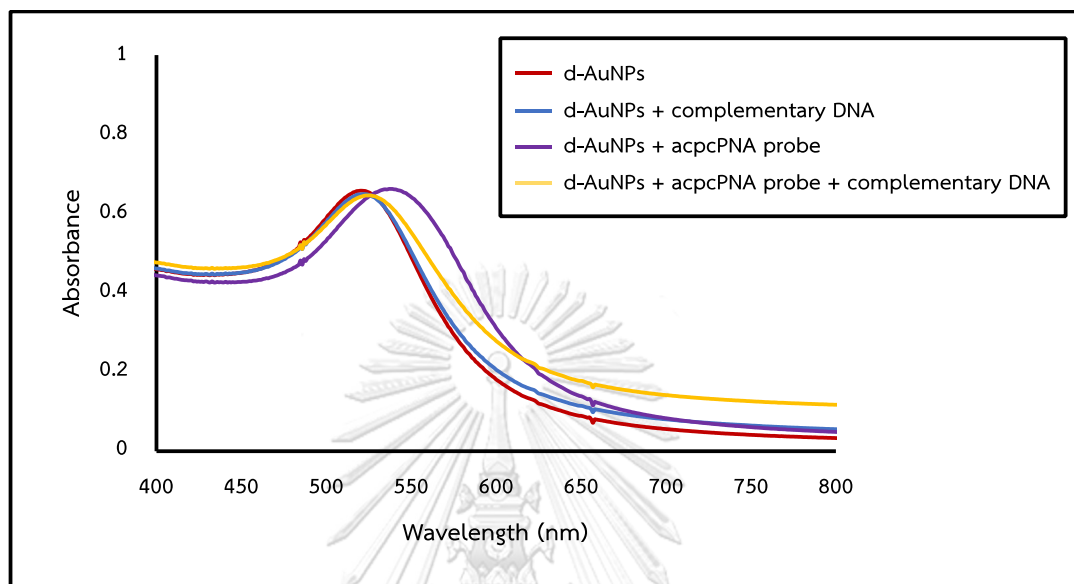
Figure 4.4 UV–vis absorption spectra of d-AuNPs with different condition

Moreover, the dispersion and morphology of d-AuNPs under each condition were investigated using transmission electron microscopy (TEM). Figure 4.5 exhibits the TEM images of d-AuNPs in different conditions. It was found that the morphology of d-AuNPs (Figure 4.5A) was spherical and the particle size of the d-AuNPs was the same as in the presence of complementary DNA (17 nm) as shown in Figure 4.5B. After adding the acpcPNA probe, the particle size of the d-AuNPs increased due to aggregation of d-AuNPs (Figure 4.5C). The results indicated that the acpcPNA probe could induce d-AuNPs aggregation while DNA could not. In addition, the particle size of the d-AuNPs in the presence of both the acpcPNA probe and the complementary DNA target was investigated. Figure 4.5D shows the mixture of small and large particle due to the presence of the d-AuNPs in both dispersion form and aggregation form. The

results from the TEM technique were consistent with the UV-vis absorption spectrophotometric technique.
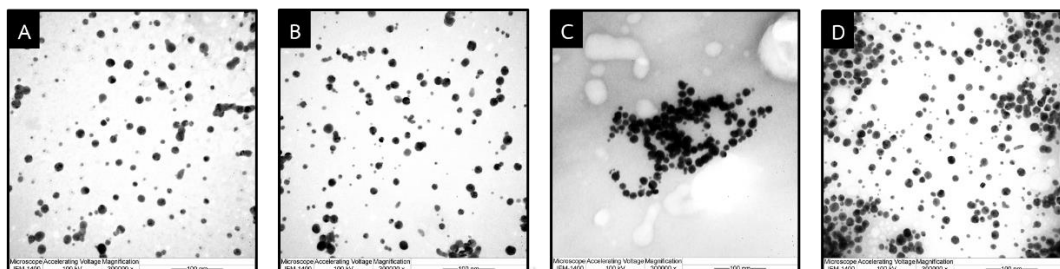
Figure 4.5 TEM images of (A) d-AuNPs, (B) d-AuNPs+DNA, (C) d-AuNPs+acpcPNA and

(D) d-AuNPs+acpcPNA +DNA

4.3 Optimization of parameters I

In order to obtain the optimal conditions, several important experimental parameters, including PBS ratio, PBS mixing time, acpcPNA probe concentration and incubation time were studied.

4.3.1 Effect of PBS ratio

The salt in the PBS which was used for the acpcPNA probe as well as DNA sample preparation steps can have a pronounced effect on the d-AuNPs aggregation. Moreover, biological samples also generally contain biological salts such as NaCl. Therefore, the effect of the PBS ratio on d-AuNPs aggregation was studied. In Figure 4.6, the color intensity from the red channel increased until the ratio of d-AuNPs:PBS reached 10:4 and tended to be stable after this point. This result indicated that beyond the ratio of d-AuNPs:PBS at 10:4, salts in the PBS solution did not affect to d-AuNPs aggregation. Hence, the ratio of 10:4 d-AuNPs:PBS was chosen for further experiments.
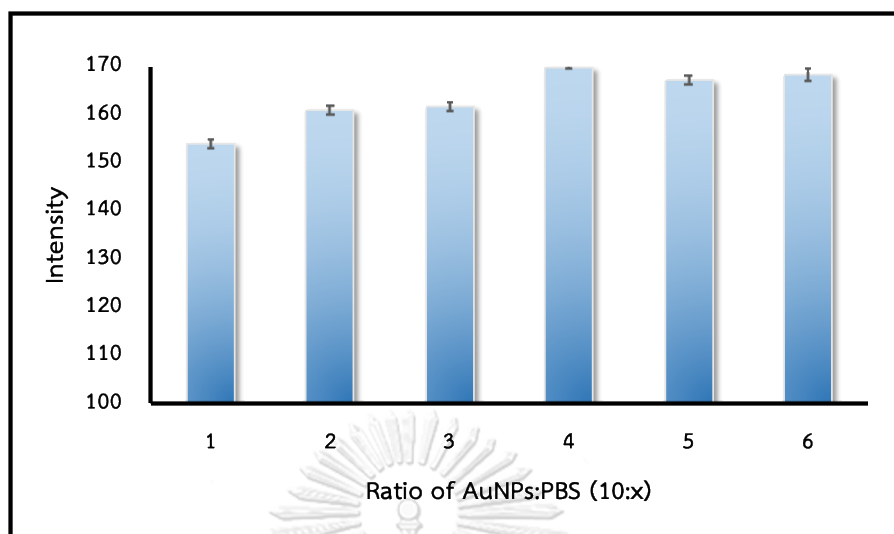
Figure 4.6 Effect of d-AuNPs:PBS buffer ratio

4.3.2 Effect of PBS mixing time

The effect of the mixing time of d-AuNPs and PBS buffer was next evaluated. The color intensity of d-AuNPs and PBS buffer mixing solution did not change when the mixing time was increased from 0 to 40 min as shown in Figure 4.7. Therefore, the d-AuNPs and PBS buffer mixing time did not affect the d-AuNPs aggregation.
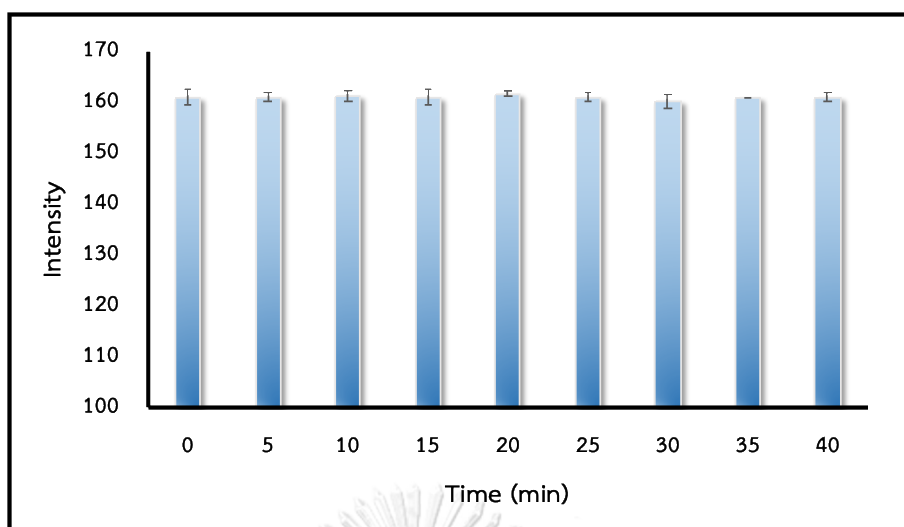
Figure 4.7 Effect of d-AuNPs and PBS mixing time between 0 to 40 min

4.3.3 acpcPNA probe concentration

Next, the effect of the acpcPNA probe concentration was investigated. We compromised between acpcPNA concentration and volume to obtain the highest intensity which means the highest degree of aggregation. The acpcPNA probe concentration and volume were varied within a range of 1 to 50 μM and 2 to 5 μL, respectively. The differential color intensity (Δ intensity) was obtained from the intensity of d-AuNPs before and after the addition of acpcPNA probe (Δ intensity = intensity $_{without\ acpcPNA\ probe}$ − intensity $_{with\ acpcPNA\ probe}$). The highest Δ intensity was observed at the concentration of 50 μM and the volume of 3 μL and tended to be stable when increasing the volume of acpcPNA as shown in Figure 4.8. At this point (3 μL of 50 μM acpcPNA probe), the aggregation of d-AuNPs was complete, resulting in the highest Δ intensity that tended to be stable beyond this point. Therefore, 50 μM acpcPNA 3 μL was selected as the optimal condition.
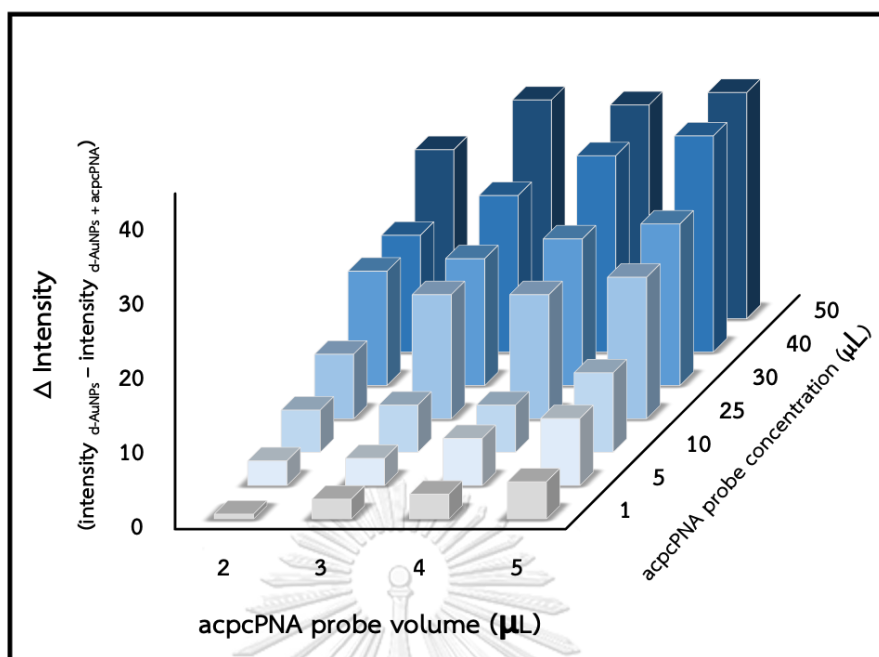
Figure 4.8 Effect of acpcPNA probe concentration and volume

4.3.4 Incubation time

The effect of incubation time in the presence of target DNA was next investigated. For this parameter, the differential color intensity (Δ intensity) obtained from the color intensity of d-AuNPs before and after addition of target DNA (Δ intensity = intensity $_{\text{with target DNA}}$ − intensity $_{\text{without target DNA}}$) decreased with the increase of incubation time and was constant after 15 min as shown in Figure 4.9. This result indicated that the reactions completely occurred after this incubation time. Therefore, 20 min of incubation time was employed for further experiments.
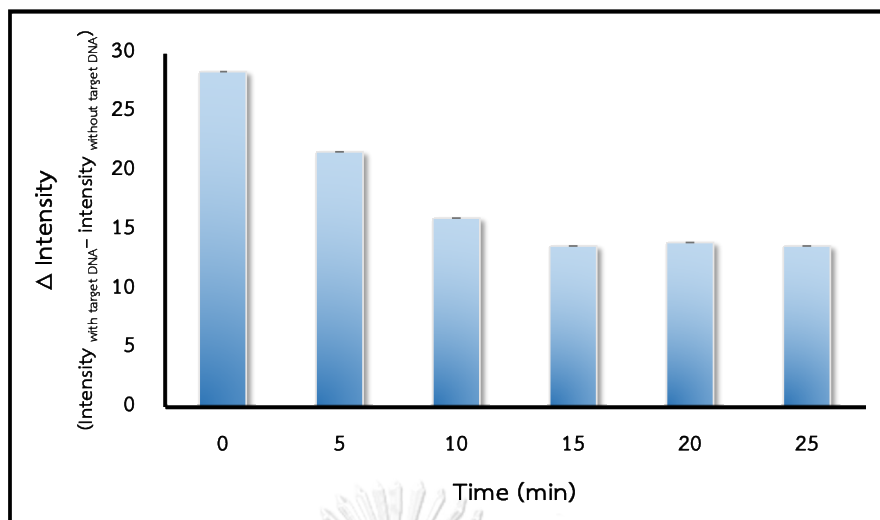
Figure 4.9 Effect of incubation time of the color intensity respond of 1 μM HPV DNA target

4.4 Analytical performance I

The analytical performance of the proposed colorimetric DNA sensor was next evaluated. Under the optimal conditions, the photographic results of the proposed colorimetric DNA sensor (Figure 4.10A), and the calibration plot between the Δ intensity (y-axis) and the concentration of the HPV DNA (x-axis) was constructed (Figure 4.10B). A linear correlation of the Δ Intensity and logarithmic DNA concentration in the range of 1 to 100 μM was observed (Figure 4.10B, inset) with a correlation coefficient (R^2) of 0.9959. The limits of detection (LODs) was found to be 1 μM from the experiment.
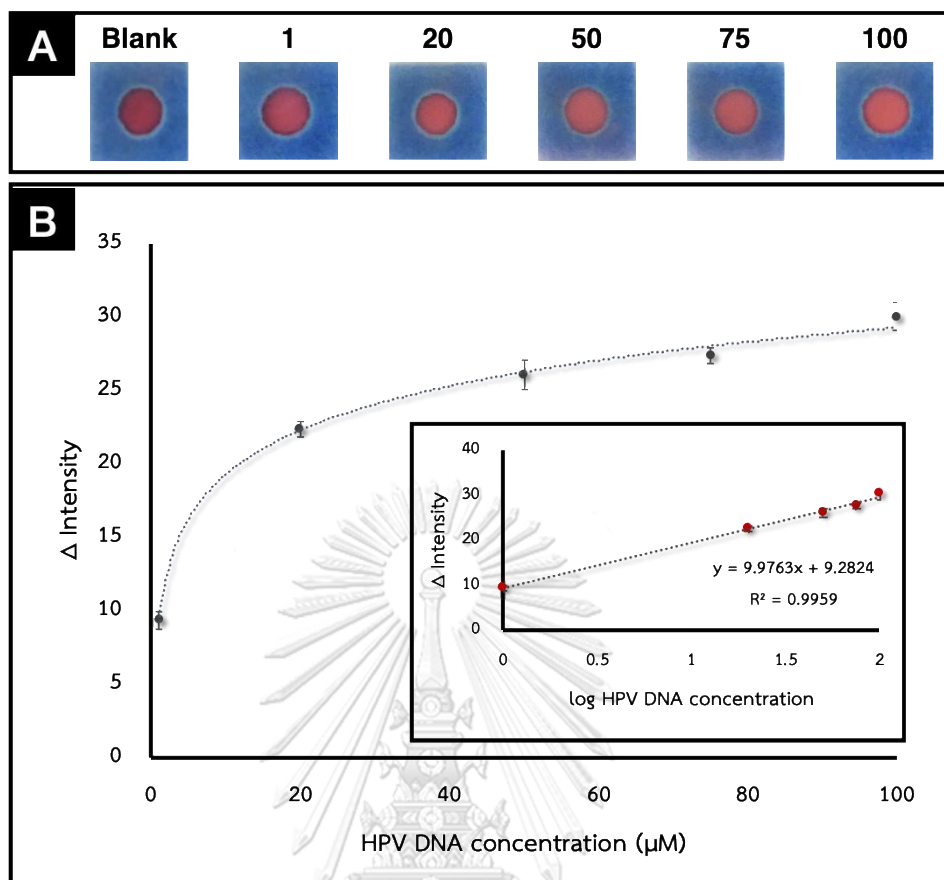
Figure 4.10 (A) Photographic results of the proposed colorimetric DNA sensor with HPV DNA concentration in the range of 1-100 µM, (B) Calibration plot between Δ Intensity vs HPV DNA concentration and calibration plot between Δ intensity and log HPV DNA concentration (inset) for HPV DNA detection

According to the obtained LOD which refers to the sensitivity of the system, the proposed concept was validated but still needs the improvement for practical applications due to the requirement of high acpcPNA probe concentrations as well as the low sensitivity at micromolar level of the target DNA that might not be sufficient for the detection of real samples (usually presented in low nanomolar levels). Due to the high stability of the d-AuNPs, a high acpcPNA probe concentration was required for inducing aggregation of the d-AuNPs to generate a visible color change. To overcome this problem, it is necessary to find a method for boosting the

aggregation of the d-AuNPs in the presence of the PNA probe in order to reduce the acpcPNA probe concentration that can detect DNA target at low concentration.

Many researches have reported about the effect of salt-induced nanoparticles aggregation. Thus, many salts such as NaCl and $MgCl_2$ have been widely used for inducing AuNPs aggregation.

In 2017, Christau and coworkers [79] reported a salt-induced aggregation of citrate-coated AuNPs confined within poly(N-isopropylacrylamide) (PNIPAM) brush structure on the substrates. When the AuNPs are confined by the PNIPAM brush structure, a red-shift and broadening of the surface plasmon band was observed because of their close vicinity. In addition, red-shift and broadening also occur due to salt-induced aggregation which is dependent on the type of salt. Different salts including NaF, NaCl, NaBr, and KCl were chosen for studying the salt-induced nanoparticles aggregation effect. The visible color change of the AuNPs from red to blue upon addition of the salt due to the increase of AuNPs aggregation was in the order NaF < NaBr < NaCl < KCl.

In 2018, Hu and coworkers [80] developed a colorimetric assay based on aptamer-modified AuNPs for determinationn of melamine in milk samples. The surface of AuNPs were functionalized with the aptamer via electrostatic interaction between the positively charged aptamers and negatively charged AuNPs. The aptamer-functionalized AuNPs provided stability to prevent the NaCl-induced aggregation. In the presence of melamine, the aptamer interacted with melamine molecules owing to decreasing of aptamer strands adsorbed on the surface of AuNPs. Then, when salt (NaCl) was presented, AuNPs aggregation occurred due to neutralize the negative charge and the color turned from red to blue. The linear range of the proposed method was found in the range of 0-1 μM with limit of detection at 22 nM.

In 2019, Huang and coworkers [81] demonstrated a dual optical sensor based on AuNPs and the duplex-specific nuclease (DSN)-assisted signal amplification technique for miRNA detection.

AuNPs were immobilized with FAM labelled hairpin probes (HPs) on the surface and the fluorescence quenching occurred via the fluorescence resonance energy transfer (FRET) mechanism. In the presence of miRNAs target, the specific hybridization of miRNAs and the DNA heteroduplexes occurred and was hydrolyzed by duplex-specific nuclease (DSN). The remarkable fluorescence recovery due to the releasing of the fluorophores into the solution. In colorimetric detection, the AuNPs with short-chain DNA were triggered $MgCl_2$, which could aggregate and color change from red to blue. They mentioned that the divalent cations displayed stronger influence of AuNPs aggregation compared with monovalent ion. The proposed method successfully detected miR-21 with the linear range of 50 pM - 1 nM and the limit of detection as low as 50 pM.

In 2020, Wang and coworkers [82] also reported a paper-based microfluidic aptasensor utilizing AuNPs for the detection of illegal drugs, including cocaine, codeine and methamphetamine. The detection principle relies on the salt-induced AuNPs aggregation to generate the color change in the presence of the target analytes. The concentration of $MgCl_2$ at 1 M was chosen as the optimal condition. In the presence of the targets, the aptamers bind to the target drug molecules and the solution containing $MgCl_2$ and sucrose moved to the AuNPs zone, causing AuNPs aggregation and color changing from red to purple. In contrast, in the absence of the target molecules, the color remained in red due to the unbound aptamers bound with the AuNPs, preventing the aggregation. The limits of detection of codeine, cocaine, and methamphetamine were found to be 3.42 µg, 3.55 µg, and 3.96 µg, respectively.

Based on these literature reviews, in order to minimize the acpcPNA probe concentration for inducing AuNPs aggregation, salts including NaCl and $MgCl_2$ were selected to investigate the interfering effects of d-AuNPs. We expected that the use of salt should lower the limit of

detection of HPV DNA by promoting the aggregation of the d-AuNPs at lower acpcPNA concentrations, hence the amounts of DNA required to prevent the aggregation should be less.

4.5 Study of salt-induced aggregation for interfering stability of d-AuNPs

NaCl and $MgCl_2$ solutions in the concentration range of 0 to 100 mM were chosen for inducing aggregation of the d-AuNPs. Figure 4.11 shows the intensity of d-AuNPs after adding NaCl and $MgCl_2$ at different concentrations for 10 min. As shown in Figure 4.11A, the color intensity of the d-AuNPs was still stable when the NaCl concentration was increased. In contrast, the intensities of the d-AuNPs clearly decreased with increasing $MgCl_2$ concentration as shown in Figure 4.11B. The result indicated that $MgCl_2$ was more effective for inducing the d-AuNPs aggregation than NaCl because the influence of divalent positive ions was stronger that monovalent ions [83]. Therefore, $MgCl_2$ was selected for further experiments.
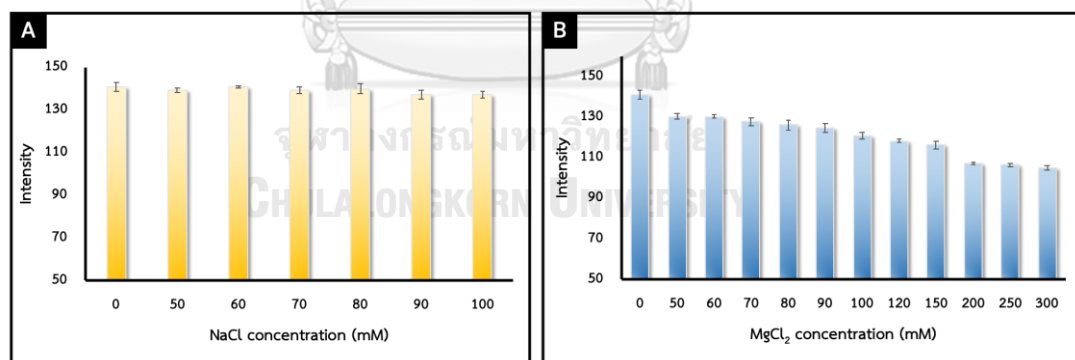
Figure 4.11 Effect of salt-induced aggregation of d-AuNPs using (A) NaCl and (B) $MgCl_2$

4.6 Optimization of parameters II

Variation of experimental parameters such as $MgCl_2$ concentration, acpcPNA probe concentration and incubation time were next investigated.

4.6.1 MgCl$_2$ and acpcPNA probe concentration

The effects of MgCl$_2$ concentrations (100-300 mM) and 2 **µ**L of acpcPNA probe concentration (1, 2, 5, and 10 **µ**M) were further investigated. It was found that the Δ intensity of 2 **µ**M acpcPNA probe with MgCl$_2$ at 100 mM (Figure 4.12, blue bar) provided the highest response when compared to other conditions. It was expected that the lower concentration of MgCl$_2$ at 100 mM did not compete with the acpcPNA probe for inducing the d-AuNPs aggregation resulting in higher Δ intensities than other conditions. In contrast, the MgCl$_2$ at 200 and 300 mM displayed lower sensitivities because the high concentrations of Mg^{2+} might induce the d-AuNPs aggregation completely, hence the acpcPNA probe cannot increase the aggregation further resulting in little color intensity change as shown in Figure 4.12 (yellow and green bar). Therefore, 2 **µ**M acpcPNA probe with 100 mM of MgCl$_2$ was selected as the optimal condition.
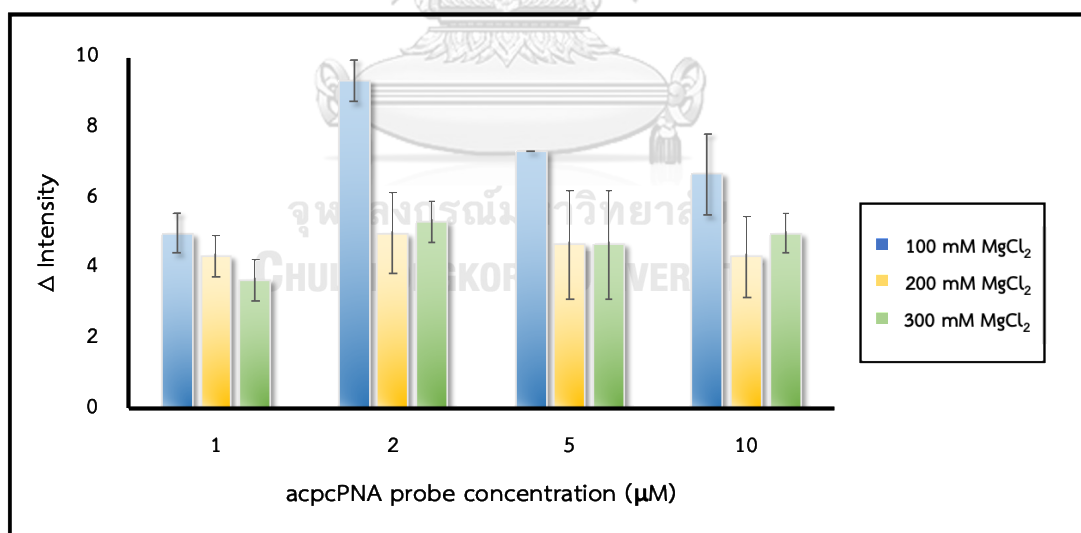
Figure 4.12 Effect of acpcPNA probe concentrations in various MgCl$_2$ conditions

4.6.2 Incubation time

To obtain the optimal reaction time, the incubation time in the range of 0 to 40 min was studied using 1 μM of the target DNA. In Figure 4.13, the Δ intensity decreased with the increasing of time and tended to be stable after 30 min., indicating the completion of the hybridization between target DNA and acpcPNA probe. Therefore, the incubation time of 30 min was seleced for further experiments.

Figure 4.13 Effect of incubation time

4.7 Analytical performance II

Different HPV DNA target concentrations were employed to evaluate the performance of the proposed DNA sensor. The Δ intensity of the d-AuNPs solution is related to the concentrations of the HPV DNA. Higher HPV DNA concentration provided higher Δ intensity as shown in Figure 4.14. Under the optimal conditions, the photographic results of the proposed colorimetric DNA sensor (Figure 4.14A) and the calibration plot between Δ intensity (y-axis) and the concentration of the HPV DNA (x-axis) (Figure 4.14B) was constructed. A good linear

relationship between the Δ Intensity and the HPV DNA concentration (logarithmic scale) were obtained in the range of 1 to 1000 nM (Figure 4.14B, inset) with a correlation coefficient (R^2) of 0.9996. The limit of detection (LOD) was found to be 1 nM from the experiment which was lower than the previously obtained LOD without adding $MgCl_2$. These results indicated that the addition of $MgCl_2$ can reduce the amount of acpcPNA probe and increase the sensitivity to the level that is sufficient for detecting HPV DNA in the biological samples.
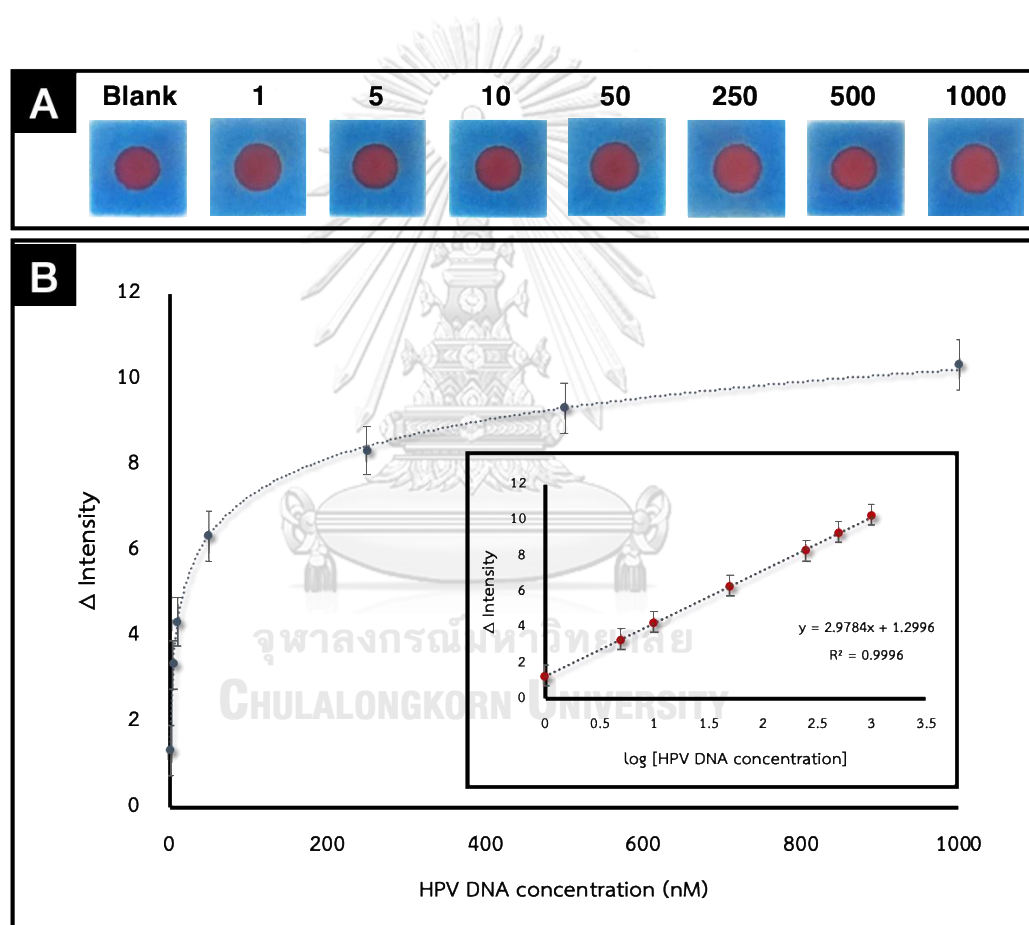
Figure 4.14 (A) Photographic results of the proposed sensor with HPV DNA concentration in the range of 1-1000 nM, (B) Δ Intensity vs HPV DNA concentration and calibration plot between Δ intensity and log HPV DNA concentration (inset) for HPV DNA detection.

4.8 Selectivity study

To investigate the selectivity of this sensor, the Δ intensity values were compared between complementary, single-base mismatch, two-base mismatch, and non-complementary DNA targets under the same experimental conditions. As shown in Figure 4.15, the complementary DNA exhibited higher Δ intensity than the single-base mismatch, two-base mismatch DNA, and non-complementary DNAs. The results showed that the proposed sensor provided a good specificity in recognizing HPV DNA, which is suitable to be applied for the HPV screening.
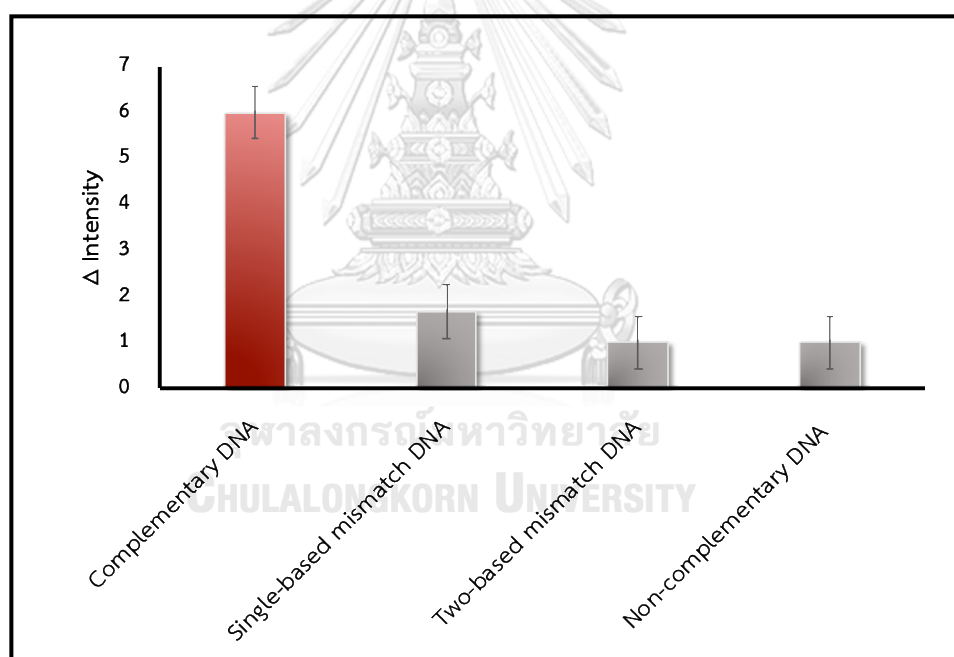
Figure 4.15 Δ Intensity of apcpPNA-induced d-AuNPs aggregation after hybridization with 50 nM of complementary DNA, 5000 nM of single-base mismatch, 5000 nM of two-base mismatch and 5000 nM of noncomplementary DNA.

4.9 Stability study

To demonstrate the stability of the proposed colorimetric HPV DNA sensor, the storage lifetime was investigated. The prepared paper-based sensor was kept at room temperature and in a refrigerator at 4 ℃. The results showed that the signal response of the sensor that kept at room temperature was stable for only 1 day whereas the signal response of the sensor kept at 4 ℃ was stable for at least 7 days, with less than 10% signal decrease as shown in Figure 4.16. It indicated that the proposed sensor has good stability for up to 7 days at 4 ℃.
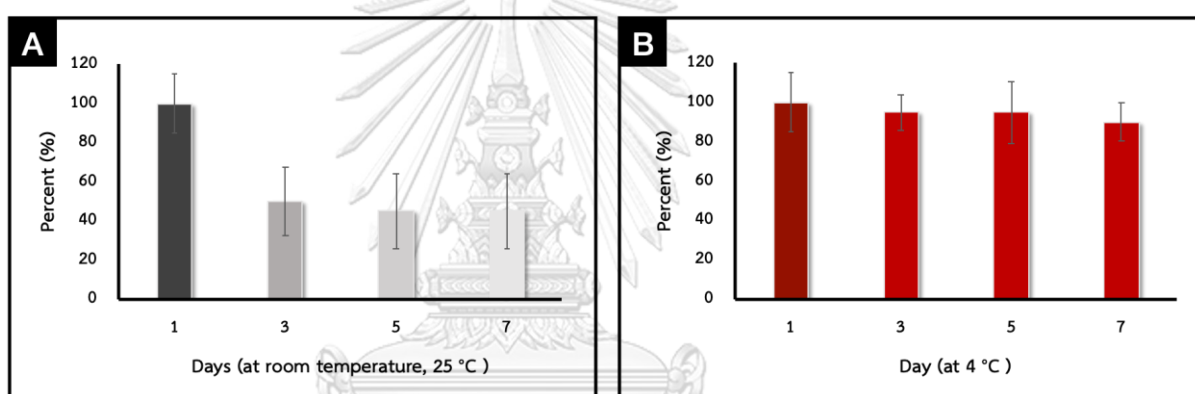
Figure 4.16 Storage lifetime of the proposed colorimetric HPV DNA sensor at room temperature (25 ℃) and 4 ℃

4.10 Real samples application

To demonstrate the applicability of the proposed sensor for the detection of real HPV DNA samples, PCR-amplified DNA from different cell lines including SiHa (HPV type 16 positive-cell line), CaSki, and C33A (HPV type 16 negative-cell line) were employed as the test samples. As expected, the positive cell line of HPV exhibited an obvious color change (expressed as Δ intensity) whereas the HPV negative-cell lines provided very small differences (Figure 4.17). In addition, a serial dilution of SiHa concentration was also evaluated to determine the

concentration-dependent signal response. The result showed that the signal tended to decrease with decreasing SiHa concentration, showing the feasibility of the proposed method for real DNA detection. As shown by these results, the proposed colorimetric DNA sensor could be successfully applied for the HPV DNA type 16 detection.
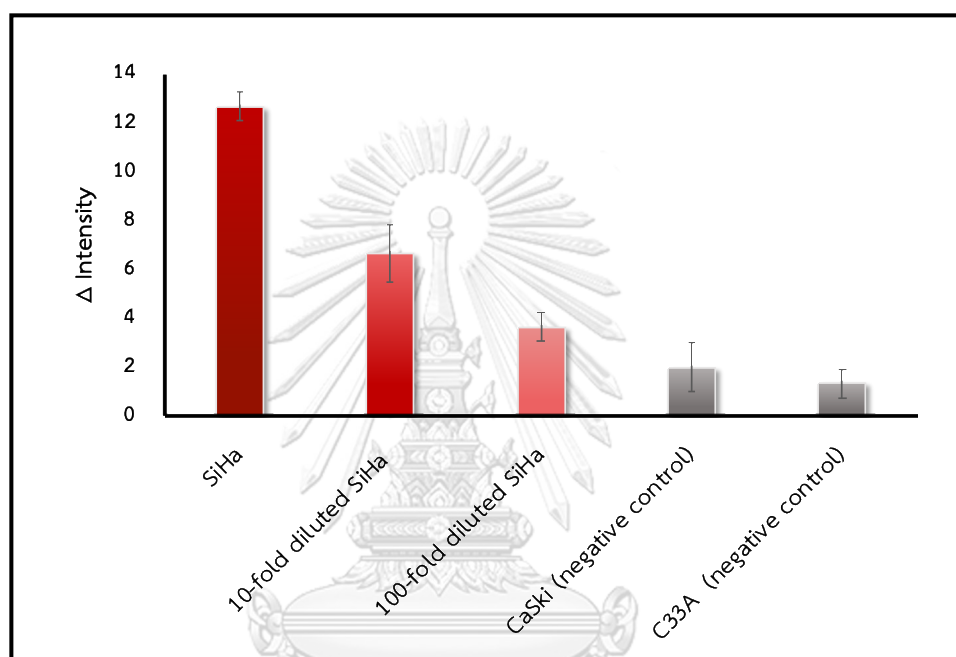
Figure 4.17 Δ Intensity of the colorimetric HPV DNA sensor in the presence of HPV type 16 positive-cell line (SiHa) and HPV type 16 negative-cell line (CaSki and C33A)

CHAPTER V

CONCLUSIONS AND FUTURE PERSPECTIVE

5.1 Conclusions

In this research, a colorimetric paper-based sensor was developed for the detection of HPV DNA. Dextrin-stabilized-AuNPs which showed good stability in salt-containing solutions was used as a colorimetric agent. The HPV DNA concentration can be quantified by monitoring the color change of the d-AuNPs upon aggregation induced by the acpcPNA probe. However, the strong stability of d-AuNPs required high concentrations of the acpcPNA probe for inducing the aggregation, resulting in poor detection limits that are unsuitable for the analysis of real samples. Therefore, $MgCl_2$ was introduced to promote the aggregation of the d-AuNPs in order to reduce the acpcPNA probe concentration, which in turn allowed the detection of the HPV DNA at lower concentrations thus providing higher sensitivity for determination. Under the optimal experimental conditions, the linear range for the detection of HPV DNA was in the range of 1 to 1000 nM with a detection limit of 1 nM from the experiment. This colorimetric DNA sensor showed high selectivity for the target DNA over single-base mismatch, two-base mismatch, and noncomplementary DNA. The sensor also showed high stability for up to 7 days at 4 °C with the percentage of the decreased signal of less than 10%. For real samples application, this developed sensor was successfully applied to detect PCR-amplified HPV DNA from cell line samples. The proposed sensor offers a simple, low-cost, and selective way to detect HPV DNA and should be useful as an alternative tool for point-of-care and economical screening of HPV for diagnosis of cervical cancer.

5.2 Future perspective

Benefitting of the modification of acpcPNA for the various DNA sensors, this DNA sensing platform can be further developed for the other HPV types as well as other infectious diseases such as tuberculosis, AIDS, etc. Moreover, the proposed device has potential to develop as a commercial device for the point-of-care screening of cervical cancer in the future.

REFERENCES

1.   Ferlay, J.; Colombet, M.; Soerjomataram, I.; Mathers, C.; Parkin, D. M.; Pineros, M.; Znaor, A.; Bray, F., Estimating the global cancer incidence and mortality in 2018: GLOBOCAN sources and methods. *Int J Cancer* **2019,** *144* (8), 1941-1953.

2.   Nicolas-Parraga, S.; Gandini, C.; Pimenoff, V. N.; Alemany, L.; de Sanjose, S.; Bosch, F. X.; Bravo, I. G.; TT, R. H.; Grp, H. V. S., HPV16 variants distribution in invasive cancers of the cervix, vulva, vagina, penis, and anus. *Cancer Medicine* **2016,** *5* (10), 2909-2919.

3.   Dyson, N.; Howley, P. M.; Munger, K.; Harlow, E., The human papilloma virus-16 E7 oncoprotein is able to bind to the retinoblastoma gene product. *Science* **1989,** *243* (4893), 934.

4.   Rolnick, S.; LaFerla, J. J.; Wehrle, D.; Trygstad, E.; Okagaki, T., Pap Smear Screening in a Health Maintenance Organization: 1986–1990. *Preventive Medicine* **1996,** *25* (2), 156-161.

5.   Cobo, F., 6 - Diagnosis of HPV infection. In *Human Papillomavirus Infections*, Cobo, F., Ed. Woodhead Publishing: 2012; pp 65-86.

6.   Clavel, C.; Masure, M.; Putaud, I.; Thomas, K.; Bory, J. P.; Gabriel, R.; Quereux, C.; Birembaut, P., Hybrid capture II, a new sensitive test for human papillomavirus detection. Comparison with hybrid capture I and PCR results in cervical lesions. *Journal of Clinical Pathology* **1998,** *51* (10), 737.

7.   Hesselink, A. T.; van Ham, M. A. P. C.; Heideman, D. A. M.; Groothuismink, Z. M. A.; Rozendaal, L.; Berkhof, J.; van Kemenade, F. J.; Massuger, L. A. F. G.; Melchers, W. J. G.; Meijer, C. J. L. M.; Snijders, P. J. F., Comparison of GP5+/6+-PCR and SPF10-line blot assays for detection of high-risk human papillomavirus in samples from women with normal cytology results who develop grade 3 cervical intraepithelial neoplasia. *Journal of clinical microbiology* **2008,** *46* (10), 3215-3221.

8.   Karbalaie Niya, M. H.; Keyvani, H.; Safarnezhad Tameshkel, F.; Salehi-Vaziri, M.; Teaghinezhad-S, S.; Bokharaei Salim, F.; Monavari, S. H. R.; Javanmard, D., Human Papillomavirus Type 16 Integration Analysis by Real-time PCR Assay in Associated

Cancers. *Translational Oncology* **2018,** *11* (3), 593-598.

9.   Fu, L. M.; Wang, Y. N., Detection methods and applications of microfluidic paper-based analytical devices. *Trac-Trends in Analytical Chemistry* **2018,** *107*, 196-211.

10.   Lim, W. Y.; Goh, B. T.; Khor, S. M., Microfluidic paper-based analytical devices for potential use in quantitative and direct detection of disease biomarkers in clinical analysis. *Journal of Chromatography B-Analytical Technologies in the Biomedical and Life Sciences* **2017,** *1060*, 424-442.

11.   Fan, Y.; Liu, J.; Wang, Y.; Luo, J.; Xu, H.; Xu, S.; Cai, X., A wireless point-of-care testing system for the detection of neuron-specific enolase with microfluidic paper-based analytical devices. *Biosensors and Bioelectronics* **2017,** *95*, 60-66.

12.   Tian, T.; Wei, X.; Jia, S.; Zhang, R.; Li, J.; Zhu, Z.; Zhang, H.; Ma, Y.; Lin, Z.; Yang, C. J., Integration of target responsive hydrogel with cascaded enzymatic reactions and microfluidic paper-based analytic devices (µPADs) for point-of-care testing (POCT). *Biosensors and Bioelectronics* **2016,** *77*, 537-542.

13.   Alba-Patiño, A.; Russell, S. M.; de la Rica, R., Origami-enabled signal amplification for paper-based colorimetric biosensors. *Sensors and Actuators B: Chemical* **2018,** *273*, 951-954.

14.   Marín-Barroso, E.; Moreira, C. M.; Messina, G. A.; Bertolino, F. A.; Alderete, M.; Soler-Illia, G. J. A. A.; Raba, J.; Pereira, S. V., Paper based analytical device modified with nanoporous material for the fluorescent sensing of gliadin content in different food samples. *Microchemical Journal* **2018,** *142*, 78-84.

15.   Liang, B.; Zhu, Q.; Fang, L.; Cao, Q.; Liang, X.; Ye, X., An origami paper device for complete elimination of interferents in enzymatic electrochemical biosensors. *Electrochemistry Communications* **2017,** *82*, 43-46.

16.   Cate, D. M.; Adkins, J. A.; Mettakoonpitak, J.; Henry, C. S., Recent developments in paper-based microfluidic devices. *Anal Chem* **2015,** *87* (1), 19-41.

17.   Wu, H.; Li, Y.; He, X.; Chen, L.; Zhang, Y., Colorimetric sensor based on 4-mercaptophenylboronic modified gold nanoparticles for rapid and selective detection of fluoride anion. *Spectrochim Acta A Mol Biomol Spectrosc* **2019,** *214*, 393-398.

18.   Yun, W.; Jiang, J. L.; Cai, D. Z.; Zhao, P. X.; Liao, J. S.; Sang, G., Ultrasensitive visual detection of DNA with tunable dynamic range by using unmodified gold

nanoparticles and target catalyzed hairpin assembly amplification. *Biosensors & Bioelectronics* **2016,** *77,* 421-427.

19.   Lin, W.-Z.; Yeung, C.-Y.; Liang, C.-K.; Huang, Y.-H.; Liu, C.-C.; Hou, S.-Y., A colorimetric sensor for the detection of hydrogen peroxide using DNA-modified gold nanoparticles. *Journal of the Taiwan Institute of Chemical Engineers* **2018,** *89,* 49-55.

20.   Shukla, R.; Bansal, V.; Chaudhary, M.; Basu, A.; Bhonde, R. R.; Sastry, M., Biocompatibility of Gold Nanoparticles and Their Endocytotic Fate Inside the Cellular Compartment: A Microscopic Overview. *Langmuir* **2005,** *21* (23), 10644-10654.

21.   Xing, S.; Xu, X.; Fu, P.; Xu, M.; Gao, T.; Zhang, X.; Zhao, C., Colorimetric detection of single base-pair mismatches based on the interactions of PNA and PNA/DNA complexes with unmodified gold nanoparticles. *Colloids Surf B Biointerfaces* **2019,** *181,* 333-340.

22.   Sassolas, A.; Leca-Bouvier, B. D.; Blum, L. J., DNA biosensors and microarrays. *Chem Rev* **2008,** *108* (1), 109-39.

23.   Wu, M. Y.; Hsu, M. Y.; Chen, S. J.; Hwang, D. K.; Yen, T. H.; Cheng, C. M., Point-of-Care Detection Devices for Food Safety Monitoring: Proactive Disease Prevention. *Trends Biotechnol* **2017,** *35* (4), 288-300.

24.   Marquez, S.; Liu, J.; Morales-Narváez, E., Paper-based analytical devices in environmental applications and their integration with portable technologies. *Current Opinion in Environmental Science & Health* **2019,** *10,* 1-8.

25.   Nielsen, P. E.; Egholm, M.; Berg, R. H.; Buchardt, O., Sequence-selective recognition of DNA by strand displacement with a thymine-substituted polyamide. *Science* **1991,** *254* (5037), 1497.

26.   Watson, J. D.; Crick, F. H. C., Molecular Structure of Nucleic Acids: A Structure for Deoxyribose Nucleic Acid. *Nature* **1953,** *171* (4356), 737-738.

27.   Vilaivan, T., Pyrrolidinyl PNA with α/β-Dipeptide Backbone: From Development to Applications. *Accounts of Chemical Research* **2015,** *48* (6), 1645-1656.

28.   Laopa, P. S.; Vilaivan, T.; Hoven, V. P., Positively charged polymer brush-functionalized filter paper for DNA sequence determination following Dot blot hybridization employing a pyrrolidinyl peptide nucleic acid probe. *Analyst* **2013,** *138*

(1), 269-277.

29. Jirakittiwut, N.; Panyain, N.; Nuanyai, T.; Vilaivan, T.; Praneenararat, T., Pyrrolidinyl peptide nucleic acids immobilised on cellulose paper as a DNA sensor. *RSC Advances* **2015,** *5* (31), 24110-24114.

30. Jampasa, S.; Siangproh, W.; Laocharoensuk, R.; Yanatatsaneejit, P.; Vilaivan, T.; Chailapakul, O., A new DNA sensor design for the simultaneous detection of HPV type 16 and 18 DNA. *Sensors and Actuators B: Chemical* **2018,** *265*, 514-521.

31. Cobo, F., 1 - Introduction and epidemiological data. In *Human Papillomavirus Infections*, Cobo, F., Ed. Woodhead Publishing: 2012; pp 1-14.

32. Toots, M.; Ustav, M., Jr.; Männik, A.; Mumm, K.; Tämm, K.; Tamm, T.; Ustav, E.; Ustav, M., Identification of several high-risk HPV inhibitors and drug targets with a novel high-throughput screening assay. *PLOS Pathogens* **2017,** *13* (2), e1006168.

33. Walboomers, J. M. M.; Jacobs, M. V.; Manos, M. M.; Bosch, F. X.; Kummer, J. A.; Shah, K. V.; Snijders, P. J. F.; Peto, J.; Meijer, C. J. L. M.; Muñoz, N., Human papillomavirus is a necessary cause of invasive cervical cancer worldwide. *The Journal of Pathology* **1999,** *189* (1), 12-19.

34. Najafov, A.; Hoxhaj, G., Chapter 1 - Introduction. In *PCR Guru*, Najafov, A.; Hoxhaj, G., Eds. Academic Press: 2017; pp 1-6.

35. Ramzan, M.; Ain, N. u.; Ilyas, S.; Umer, M.; Bano, S.; Sarwar, S.; Shahzad, N.; Shakoori, A. R., A cornucopia of screening and diagnostic techniques for human papillomavirus associated cervical carcinomas. *Journal of Virological Methods* **2015,** *222*, 192-201.

36. Martinez, A. W.; Phillips, S. T.; Butte, M. J.; Whitesides, G. M., Patterned paper as a platform for inexpensive, low-volume, portable bioassays. *Angew Chem Int Ed Engl* **2007,** *46* (8), 1318-1320.

37. Wu, G.; Zaman, M. H., Low-cost tools for diagnosing and monitoring HIV infection in low-resource settings. *Bull World Health Organ* **2012,** *90* (12), 914-920.

38. Carrilho, E.; Phillips, S. T.; Vella, S. J.; Martinez, A. W.; Whitesides, G. M., Paper Microzone Plates. *Analytical Chemistry* **2009,** *81* (15), 5990-5998.

39. Maejima, K.; Tomikawa, S.; Suzuki, K.; Citterio, D., Inkjet printing: an integrated and green chemical approach to microfluidic paper-based analytical devices. *RSC*

Advances **2013,** *3* (24), 9258-9263.

40.   Kao, P.-K.; Hsu, C.-C., One-step rapid fabrication of paper-based microfluidic devices using fluorocarbon plasma polymerization. *Microfluidics and Nanofluidics* **2014,** *16* (5), 811-818.

41.   Lu, Y.; Shi, W.; Jiang, L.; Qin, J.; Lin, B., Rapid prototyping of paper-based microfluidics with wax for low-cost, portable bioassay. *ELECTROPHORESIS* **2009,** *30* (9), 1497-1500.

42.   Sameenoi, Y.; Nongkai, P. N.; Nouanthavong, S.; Henry, C. S.; Nacapricha, D., One-step polymer screen-printing for microfluidic paper-based analytical device (μPAD) fabrication. *Analyst* **2014,** *139* (24), 6580-6588.

43.   Nie, J.; Liang, Y.; Zhang, Y.; Le, S.; Li, D.; Zhang, S., One-step patterning of hollow microstructures in paper by laser cutting to create microfluidic analytical devices. *Analyst* **2013,** *138* (2), 671-676.

44.   Dhar, P., Measuring tobacco smoke exposure: quantifying nicotine/cotinine concentration in biological samples by colorimetry, chromatography and immunoassay methods. *Journal of Pharmaceutical and Biomedical Analysis* **2004,** *35* (1), 155-168.

45.   Han, L.; Liu, S. G.; Liang, J. Y.; Li, N. B.; Luo, H. Q., Free-label dual-signal responsive optical sensor by combining resonance Rayleigh scattering and colorimetry for sensitive detection of glutathione based on ultrathin MnO2 nanoflakes. *Sensors and Actuators B: Chemical* **2019,** *288,* 195-201.

46.   Wongthanyakram, J.; Harfield, A.; Masawat, P., A smart device-based digital image colorimetry for immediate and simultaneous determination of curcumin in turmeric. *Computers and Electronics in Agriculture* **2019,** *166,* 104981.

47.   Yang, Q.; Wang, X.; Peng, H.; Arabi, M.; Li, J.; Xiong, H.; Choo, J.; Chen, L., Ratiometric fluorescence and colorimetry dual-mode assay based on manganese dioxide nanosheets for visual detection of alkaline phosphatase activity. *Sensors and Actuators B: Chemical* **2020,** *302,* 127176.

48.   Luo, X.; Xie, X.; Meng, Y.; Sun, T.; Ding, J.; Zhou, W., Ligands dissociation induced gold nanoparticles aggregation for colorimetric Al3+ detection. *Analytica Chimica Acta* **2019,** *1087,* 76-85.

49.   Xue, X.; Gao, M.; Rao, H.; Luo, M.; Wang, H.; An, P.; Feng, T.; Lu, X.; Xue, Z.; Liu, X., Photothermal and colorimetric dual mode detection of nanomolar ferric ions in environmental sample based on in situ generation of prussian blue nanoparticles. *Analytica Chimica Acta* **2020,** *1105,* 197-207.

50.   Akshaya, K.; Arthi, C.; Pavithra, A. J.; Poovizhi, P.; Antinate, S. S.; Hikku, G. S.; Jeyasubramanian, K.; Murugesan, R., Bioconjugated gold nanoparticles as an efficient colorimetric sensor for cancer diagnostics. *Photodiagnosis and Photodynamic Therapy* **2020,** *30,* 101699.

51.   Li, Z.-M.; Pi, T.; Yan, X.-L.; Tang, X.-M.; Deng, R.-H.; Zheng, X.-J., Label-free and enzyme-free one-step rapid colorimetric detection of DNA methylation based on unmodified gold nanoparticles. *Spectrochimica Acta Part A: Molecular and Biomolecular Spectroscopy* **2020**, 118375.

52.   Rostami, S.; Mehdinia, A.; Niroumand, R.; Jabbari, A., Enhanced LSPR performance of graphene nanoribbons-silver nanoparticles hybrid as a colorimetric sensor for sequential detection of dopamine and glutathione. *Analytica Chimica Acta* **2020,** *1120,* 11-23.

53.   Zhu, X.; Gao, T., Chapter 10 - Spectrometry. In *Nano-Inspired Biosensors for Protein Assay with Clinical Applications*, Li, G., Ed. Elsevier: 2019; pp 237-264.

54.   Zhao, W.; Brook, M. A.; Li, Y., Design of Gold Nanoparticle-Based Colorimetric Biosensing Assays. *ChemBioChem* **2008,** *9* (15), 2363-2371.

55.   António, M.; Ferreira, R.; Vitorino, R.; Daniel-da-Silva, A. L., A simple aptamer-based colorimetric assay for rapid detection of C-reactive protein using gold nanoparticles. *Talanta* **2020,** *214,* 120868.

56.   Lapenna, A.; Dell'Aglio, M.; Palazzo, G.; Mallardi, A., "Naked" gold nanoparticles as colorimetric reporters for biogenic amine detection. *Colloids and Surfaces A: Physicochemical and Engineering Aspects* **2020,** *600,* 124903.

57.   Moradi, M.; Sohrabi, M. R.; Mortazavinik, S., Simultaneous ultra-trace quantitative colorimetric determination of antidiabetic drugs based on gold nanoparticles aggregation using multivariate calibration and neural network methods. *Spectrochimica Acta Part A: Molecular and Biomolecular Spectroscopy* **2020,** *234,* 118254.

58.   Baetsen-Young, A. M.; Vasher, M.; Matta, L. L.; Colgan, P.; Alocilja, E. C.; Day, B., Direct colorimetric detection of unamplified pathogen DNA by dextrin-capped gold nanoparticles. *Biosensors and Bioelectronics* **2018,** *101*, 29-36.

59.   Wang, Y.; Zhan, L.; Huang, C. Z., One-pot preparation of dextran-capped gold nanoparticles at room temperature and colorimetric detection of dihydralazine sulfate in uric samples. *Analytical Methods* **2010,** *2* (12), 1982-1988.

60.   Katti, K. K.; Kattumuri, V.; Bhaskaran, S.; Katti, K. V.; Kannan, R., Facile and General Method for Synthesis of Sugar-Coated Gold Nanoparticles. *International Journal of Green Nanotechnology: Biomedicine* **2009,** *1* (1), B53-B59.

61.   Pray, L. A., Discovery of DNA structure and function: Watson and Crick. *Nature Education* **2008,** *1* (1), 100.

62.   Miao, Y.; Wang, R.; Yang, W.; Liu, S.; Yan, G., Detection of biological mercaptan by DNA functionalized room temperature phosphorescent quantum dot nanocomposites. *Spectrochimica Acta Part A: Molecular and Biomolecular Spectroscopy* **2020,** *238*, 118420.

63.   Jung, Y. K.; Park, H. G., Colorimetric detection of clinical DNA samples using an intercalator-conjugated polydiacetylene sensor. *Biosensors and Bioelectronics* **2015,** *72*, 127-132.

64.   Zubakov, D.; Chamier-Ciemińska, J.; Kokmeijer, I.; Maciejewska, A.; Martínez, P.; Pawłowski, R.; Haas, C.; Kayser, M., Introducing novel type of human DNA markers for forensic tissue identification: DNA copy number variation allows the detection of blood and semen. *Forensic Science International: Genetics* **2018,** *36*, 112-118.

65.   Egholm, M.; Buchardt, O.; Christensen, L.; Behrens, C.; Freier, S. M.; Driver, D. A.; Berg, R. H.; Kim, S. K.; Norden, B.; Nielsen, P. E., PNA hybridizes to complementary oligonucleotides obeying the Watson–Crick hydrogen-bonding rules. *Nature* **1993,** *365* (6446), 566-568.

66.   Pellestor, F.; Paulasova, P., The peptide nucleic acids (PNAs), powerful tools for molecular genetics and cytogenetics. *European Journal of Human Genetics* **2004,** *12* (9), 694-700.

67.   Wang, J.; Palecek, E.; Nielsen, P. E.; Rivas, G.; Cai, X.; Shiraishi, H.; Dontha, N.;

Luo, D.; Farias, P. A. M., Peptide Nucleic Acid Probes for Sequence-Specific DNA Biosensors. *Journal of the American Chemical Society* **1996,** *118* (33), 7667-7670.

68.   Jampasa, S.; Wonsawat, W.; Rodthongkum, N.; Siangproh, W.; Yanatatsaneejit, P.; Vilaivan, T.; Chailapakul, O., Electrochemical detection of human papillomavirus DNA type 16 using a pyrrolidinyl peptide nucleic acid probe immobilized on screen-printed carbon electrodes. *Biosensors and Bioelectronics* **2014,** *54,* 428-434.

69.   Jimenez Jimenez, A. M.; Rodrigo, M. A. M.; Milosavljevic, V.; Krizkova, S.; Kopel, P.; Heger, Z.; Adam, V., Gold nanoparticles-modified nanomaghemite and quantum dots-based hybridization assay for detection of HPV. *Sensors and Actuators B: Chemical* **2017,** *240,* 503-510.

70.   Choleva, T. G.; Kappi, F. A.; Giokas, D. L.; Vlessidis, A. G., Paper-based assay of antioxidant activity using analyte-mediated on-paper nucleation of gold nanoparticles as colorimetric probes. *Analytica Chimica Acta* **2015,** *860,* 61-69.

71.   Aydindogan, E.; Ceylan, A. E.; Timur, S., Paper-based colorimetric spot test utilizing smartphone sensing for detection of biomarkers. *Talanta* **2020,** *208,* 120446.

72.   Liu, Y.; Li, T.; Ling, C.; Wang, Z.; Jin, L.; Zhao, Y.; Chen, Z.; Li, S.; Deng, Y.; He, N., A simple visual method for DNA detection based on the formation of gold nanoparticles. *Chinese Chemical Letters* **2019,** *30* (12), 2359-2362.

73.   Kanjanawarut, R.; Su, X., Colorimetric Detection of DNA Using Unmodified Metallic Nanoparticles and Peptide Nucleic Acid Probes. *Analytical Chemistry* **2009,** *81* (15), 6122-6129.

74.   Su, X.; Kanjanawarut, R., Control of Metal Nanoparticles Aggregation and Dispersion by PNA and PNA–DNA Complexes, and Its Application for Colorimetric DNA Detection. *ACS Nano* **2009,** *3* (9), 2751-2759.

75.   Teengam, P.; Siangproh, W.; Tuantranont, A.; Vilaivan, T.; Chailapakul, O.; Henry, C. S., Multiplex Paper-Based Colorimetric DNA Sensor Using Pyrrolidinyl Peptide Nucleic Acid-Induced AgNPs Aggregation for Detecting MERS-CoV, MTB, and HPV Oligonucleotides. *Analytical Chemistry* **2017,** *89* (10), 5428-5435.

76.   Jirakittiwut, N.; Munkongdee, T.; Wongravee, K.; Sripichai, O.; Fucharoen, S.; Praneenararat, T.; Vilaivan, T., Visual genotyping of thalassemia by using pyrrolidinyl peptide nucleic acid probes immobilized on carboxymethylcellulose-modified paper

and enzyme-induced pigmentation. *Microchimica Acta* **2020,** *187* (4), 238.

77.   Vilaivan, T.; Srisuwannaket, C., Hybridization of Pyrrolidinyl Peptide Nucleic Acids and DNA: Selectivity, Base-Pairing Specificity, and Direction of Binding. *Organic Letters* **2006,** *8* (9), 1897-1900.

78.   Katti, K. K.; Kattumuri, V.; Bhaskaran, S.; Katti, K. V.; Kannan, R., Facile and General Method for Synthesis of Sugar Coated Gold Nanoparticles. *Int J Green Nanotechnol Biomed* **2009,** *1* (1), B53-B59.

79.   Christau, S.; Moeller, T.; Genzer, J.; Koehler, R.; von Klitzing, R., Salt-Induced Aggregation of Negatively Charged Gold Nanoparticles Confined in a Polymer Brush Matrix. *Macromolecules* **2017,** *50* (18), 7333-7343.

80.   Hu, X.; Chang, K.; Wang, S.; Sun, X.; Hu, J.; Jiang, M., Aptamer-functionalized AuNPs for the high-sensitivity colorimetric detection of melamine in milk samples. *PLOS ONE* **2018,** *13* (8), e0201626.

81.   Huang, J.; Shangguan, J.; Guo, Q.; Ma, W.; Wang, H.; Jia, R.; Ye, Z.; He, X.; Wang, K., Colorimetric and fluorescent dual-mode detection of microRNA based on duplex-specific nuclease assisted gold nanoparticle amplification. *Analyst* **2019,** *144* (16), 4917-4924.

82.   Wang, L.; McCord, B., A four-channel paper microfluidic device with gold nanoparticles and aptamers for seized drugs. *Analytical Biochemistry* **2020,** *595*, 113619.

83.   Liu, T.; Zhao, J.; Zhang, D.; Li, G., Novel Method to Detect DNA Methylation Using Gold Nanoparticles Coupled with Enzyme-Linkage Reactions. *Analytical Chemistry* **2010,** *82* (1), 229-233.

VITA

NAME   Sarida Naorungroj

DATE OF BIRTH   14 May 1996

PLACE OF BIRTH   Phetchaburi

INSTITUTIONS ATTENDED   Chulalongkorn University

HOME ADDRESS   353/1 Moo 4 Banmor, Mueang Phetchaburi District,
                         Phetchaburi 76000

PUBLICATION   Proceeding:
                         Sarida Naorungroj, Prinjaporn Teengam, Tirayut Vilaivan,
                         Orawon Chailapakul "Development of paper-based
                         colorimetric sensor for determination of Human
                         Papillomavirus DNA" The Pure and Applied Chemistry
                         International Conference 2020 - PACCON 2020 Chemistry
                         for Catalyzing Sustainability and Prosperity, IMPACT Forum,
                         Mauangthong Thani, Bangkok, Thailand, February 13-14,
                         2020, pp 1-7.

จุฬาลงกรณ์มหาวิทยาลัย
CHULALONGKORN UNIVERSITY